46TH TURBOMACHINERY & 33RD PUMP SYMPOSIA
HOUSTON, TEXAS | SEPTEMBER 11 – 14, 2017
GEORGE R. BROWN CONVENTION CENTER

CENTRIFUGAL COMPRESSOR PERFORMANCE MAKING ENLIGHTENED ANALYSIS DECISIONS

B. Fred Evans, P.E.
Lead Rotating Machinery Engineer
Chiyoda International Corp.
Houston, TX, USA

Spencer Huble
Rotating Machinery Engineer
Chiyoda International Corp.
Houston, TX, USA

B. Fred Evans is Lead Rotating Machinery Engineer for Chiyoda International Corporation in Houston, Texas. His experience includes machinery related projects for ExxonMobil Development Company, Shell Global Solutions, BP, Amoco, and Southwest Research Institute. Mr. Evans has provided machinery engineering services and field technical troubleshooting for dynamics problems. Mr. Evans received BSME and MSME Degrees from Texas Tech University. He is a Life Member of ASME and is a registered Professional Engineer in the State of Texas.

Spencer R. Huble is a Rotating Machinery Engineer with Chiyoda International Corporation in Houston, Texas. His current duties involve specifying, selecting, procuring, and testing of new rotating equipment, primarily in downstream oil and gas applications. Prior to joining Chiyoda, he was employed by S&B Engineers and Constructors. Mr. Huble received his BSME Degree from The University of Texas at Austin (2014).

ABSTRACT

Historical background of centrifugal compressor aerodynamic analysis development introduces eight calculation methods for polytropic performance. The results are shown via a direct comparison of examples illustrating trends. The small stage method is shown to be a highly accurate, easy to implement, real gas alternative to current test code methods. Additionally, the importance of understanding fluid properties as they relate to compressor performance is illustrated.

INTRODUCTION

At the heart of many hydrocarbon gas processing schemes is a centrifugal compressor that must provide a specified mass flow and head to circulate a fluid through a facility. In so doing, the fluid's total (stagnation) thermodynamic state is changed from a suction to a discharge state by the compressor. Determining the required power to drive a compressor at design conditions as well as at off design operating points facilitates driver sizing and selection. Flow, head, and efficiency curves of a particular aerodynamic compressor design are provided to a client and guaranteed by a vendor for a project's design, usually during the purchasing stage of a project. At the conclusion of manufacturing, thermodynamic testing is carried out to prove a machine will meet the contractually guaranteed performance. A client engineer's performance acceptance decision can be impacted by variations between design versus as tested performance parameter values. Tools to assist client engineers when independently calculating performance should be clear as to the methods employed and any imposed limitations. This facilitates understanding comparisons to the manufacturer's test reports. These tools can include expensive process simulators, custom proprietary applications, and spreadsheets with built in equation of state access.

Caution – Models In Use

It is common industry practice to employ mathematical models to provide performance evaluations based upon measured compressor operating parameters. Models for determination of compressor head as well as fluid equations of state (EOS) models are based upon underlying assumptions that must be considered. Thus, while studying compressor performance, it is important to remember that these models do not necessarily provide exact replicas of the systems studied. Quotes from two statisticians may serve to set the tone for how models could be regarded.

> *"Remember that all models are wrong; the practical question is how wrong do they have to be to not be useful." (Box and Draper, 1987)*
>
> *"All models are right…most are useless." (Tarpey, 2009)*

On the surface, the quotes seem to be in conflict, however, when the source references are studied, it is evident that they both have a similar meaning from different points of view, and are analogous to *is a glass half full or half empty*. Models are limited by theoretical assumptions required to create them. In discussions of compressor performance, the expectation is that models would give a fair representation of a compressors' ability to meet quoted performance. Models must not be taken out of context which requires an analyst to study results in light of underlying assumptions. Some of the methods (models) discussed below are based upon assumptions that sometimes get overlooked which can introduce the potential for excessive errors that should be avoided.

Testing Error Sources

Centrifugal compressor performance test results can be negatively impacted in four principle realms assuming the machine has been properly built and installed on the test stand or in the field. Each of these is shown in Table 1 with comments. The first two are extremely important but are beyond the scope of this paper. The third is given limited fundamental discussion. Many good references can be found in the open technical literature that address these three issues. The fourth issue is the main current subject.

Table 1: Issues Impacting Centrifugal Compressor Performance Test Results

Performance Impact Issue	Comments
Measured Data Inaccuracy (locations, pressures, temperatures, flows, speed)	• Extensively addressed in ASME PTC 10 • Actively managed by proper quality control techniques • Importance of suction state conditions in relation to a fluid's two phase region boundary • Uncertainty can be quantified
Fluid Composition Determination (species, precision of mole percentages)	• Differences between design and field compositions • Better controlled on test stand than in field • Sufficient measurement technology exists but can be expensive • Transportation logistics hampers timely results
Thermodynamic Equation of State (availability, applicability, accuracy, precision)	• Simple and complex versions and implementations available • Accuracy and ease of access currently sufficient • Consistency between all parties involved recommended • Proper equation selection requires knowledge of specific fluids and conditions for test and design
Polytropic Performance Calculation Method (What is really being calculated?, assumptions)	• Accuracy can depend upon specific fluid and conditions • Ideal gas vs. real gas assumptions impact results • Current code approximations developed when computing facilities were limited • Highly accurate methods are available yet simple • Intended use impacts selection of method

This discussion will address various methods employed for interpretation of steady state performance test data for an uncooled, single stage of compression that may include multiple impellers, i.e. a flow path from suction flange to discharge flange without side streams. The required minimum input data to estimate compressor stage head and efficiency consists of two fluid state point variables (usually pressure and temperature) at both suction and discharge locations and the fluid composition. Additional restrictions for this discussion are that the compressed fluid is a single gaseous phase and that stagnation properties have been determined. The American Society of Mechanical Engineers Power Test Code (ASME PTC 10, 1997) prescribes strict regimens for obtaining valid test measurements and it is assumed for the calculations discussed in this paper that the data has been properly obtained and averaged accordingly. Application of the eight methods compared in this paper will be restricted to using this minimum data. Further performance information can be determined if mass flow rate and compressor speed/geometry data are available, but those calculations, while very important, are fairly straight forward and beyond the primary focus of this paper.

Dealing with Test Results

Consistent, accurate methods to calculate flange to flange centrifugal compressor polytropic performance are required to evaluate a machine's thermodynamic acceptance guarantees. These guarantees are typically listed in project purchase documents by reference to an industry accepted code, but only mention general details of implementation. An original equipment manufacturer (OEM) uses internally developed standard testing procedures and methods and provides test results to a client based upon them. These vendor procedures are rigorously controlled for consistency across a product line. When a client develops an independent determination of performance test results that yields answers different from the OEM that may exceed specified tolerances, resolution can be difficult since it may involve technical as well as contractual aspects. By this time it is usually too late in a project's schedule to make any hardware changes without additional costs and long delays. The time to address performance determination methods is before a contract is signed, not after test stand results are brought into question. It may seem less important during the period of contract negotiations, but writing details into a clause in the contract can help avoid problems or help deal with them efficiently later.

Having a clear understanding of why various performance calculations can yield different results from the same input data can go a long way in resolving test stand issues. The origin of differing thermodynamic performance calculation results can usually be traced to seemingly minor variations in developing polytropic exponents, real gas correction factors, gas properties determined from various equations of state, and occasionally, the very definition of efficiency. This paper provides a comparative numerical evaluation of eight methods for calculation of centrifugal compressor thermodynamic fluid performance. To maintain the focus of this paper upon methods and their underlying assumptions, calculations of example cases by the eight methods are based upon a single, well referenced implementation of multiple, pure fluid, reference quality equations of state and fluid component mixing rules (Lemmon, et al., 2013).

Compressor testing can take many forms to which these calculation methods can be applied. The most common testing scenario occurs at the manufacturer's facility just prior to hardware shipment when the compressor must be shown to meet design requirements. Due to facility limitations and safety precautions, performance testing does not typically duplicate field design conditions but is based upon aerodynamic similitude employing inert gases, typically at lower than design pressures and power (O'Neill and Wickli, 1962; Key, 1989). Consequently, performance calculation methods that are sufficient for processing test stand measured data may not be as applicable for field measured data.

Power Test Code

The Power Test Code (ASME PTC 10, 1997) provides a framework for centrifugal compressor testing and prescribes allowable testing tolerances. Maintaining test results within these tolerances is intended to allow conversion for comparison to project specified design conditions via similitude. The code is meant to assure an accurate test result but does not directly address technical acceptability of a compressor to meet contractual requirements. In other words, adherence to the code helps perform a good test that is representative of a particular machine's capability. Further evaluation of achieving contractual guarantees is not the intent of the power test code as those are governed by contractual documents and typically tolerances found in API Standard 617 (2014).

Within the code framework, the processing of measured test stand data can be accomplished by the choice of three methods. The most commonly applied is based upon a classic technical paper (Schultz, 1962) that derived real gas thermodynamic relations for the compression process using suction and discharge end point fluid states and a correction factor derived from isentropic considerations. Two methods for determining polytropic exponents were defined in Schultz's paper along with an example case. The Schultz methodology was adapted and incorporated into the ASME PTC 10 code in 1965 and reaffirmed in 1997 and has been employed by

many users when purchasing compressors. However, exact rules for implementation within the test code are not provided for all aspects, leaving the door open for a certain amount of interpretation such as mentioned in code Section 5.2. Assumptions employed by Schultz to arrive at a solution can be shown to cause inaccuracies beyond acceptable limits in some applications.

Over the ensuing years since first introduced, several technical papers have offered comments, refinements, improvements and/or alternatives to the Schultz methods (Mallen and Saville, 1977; Nathoo and Gottenberg, 1981, 1983; Huntington, 1985, 1997; Hunseid, et al. 2006; Oldrich, 2010; Sandberg and Colby, 2013; Taher, 2014; Wettstein, 2014; Plano, 2014; Evans and Huble, 2017). Also during this time, the determination of real gas properties via thermodynamic equations of state has vastly expanded in quantity and quality, as well as ease of access and use. When the Schultz method was first embraced by the PTC 10 code, availability of computing power was a mere shadow of what it is today. Performance calculation methods no longer need be hampered by simplifying techniques since robust numerical manipulation requires only inexpensive yet powerful resources that are readily available to any analyst.

Path Work – Efficiency

A basic fact of thermodynamics is that the work required to compress a gas from one state to a higher pressure state is path dependent. Thus, the required shaft work input to a centrifugal compressor to compress a fluid from $P_S,T_S \rightarrow P_D,T_D$ depends on the thermodynamic compression path that the fluid undergoes. Two commonly discussed reference compression paths between two pressure levels are isentropic and polytropic. The current discussion deals with estimation of polytropic compression which can be defined as a process which occurs with an interchange of both heat and work between a system and its surroundings. Teaching of gas state thermodynamics in secondary education begins with the concept of an ideal or perfect gas model whereas fluids encountered in the turbocompressor industry may not be adequately represented by those concepts. It is important to identify the thermodynamic definitions associated with gas model labels (Oldrich, 2010). Table 2 provides a high level overview of three models. In reviewing applicable literature, one should take note of the gas model assumptions employed by each author and particularly take note if they are not stated.

Table 2: Fluid Gas Models

Model	Treatment of Z and Cp	Equation of State
Perfect Gas	Z = 1 Cp = Constant	Pv = RT
Ideal Gas	Z = 1 Cp = function of temperature only	Pv = RT
Real Gas	Z and Cp function of temperature and pressure	Pv = ZRT

The perfect gas model is not necessarily useful for application to the current subject but the label is sometimes used interchangeably with the ideal gas model in engineering literature. Early work in the subject field that led to the ideal gas relationships between volume, temperature, and pressure was conducted at relatively low pressures and moderate temperatures which allowed reasonable results to be obtained with the perfect gas model. In today's environment, real gas concepts are usually required and will be addressed in this paper. They can also provide accurate results for gases that could be dealt with by ideal gas concepts.

To determine centrifugal compressor polytropic performance, it is necessary to calculate efficiency. Following a different compression path will yield a different efficiency. Efficiency can be an elusive term. For purposes of the subject calculations, efficiency is assumed constant throughout the compression process, but this does not limit the validity of the results. This is true since it is an overall machine efficiency that is of interest during contractual performance testing rather than the efficiencies of individual internal parts.

Efficiency can be defined as the ratio of useful polytropic compression work to the total energy absorbed by the compressor. The measure of compression work is referred to as polytropic head while the total energy is measured by the change in total (stagnation) enthalpy of the fluid between suction and discharge states regardless of path. Evaluation of methods to calculate the former is the main subject of this paper while the later (ΔH) is usually provided by an applicable fluid equation of state. For purposes of clarity, casing heat flow to the surroundings, end seal leakage, and mechanical losses are not included in the present thermodynamic discussion but must be considered when evaluating test stand results since all will impact overall efficiency.

Methods

Evaluation of compressor thermodynamic performance comes down to determining the compression path and associated polytropic head. While no calculation method can be claimed to be exact for a real gas, multiple estimation methods have been put forward that

have served the industry. Two broad categories of methods can be defined as 1) using fluid compression end point states with or without a correction factor and 2) numerical techniques consisting of calculations at multiple small compression pressure steps between the end point fluid states. Many of the methods require some form of trial and error iteration. Comparing implementation of the various methods and their relative accuracy can be insightful, especially to a novice trying to get his head around the entire performance concept.

There are eight head calculation methods compared in this paper with multiple implementations of two of the numerical methods. Three other methods reported in the relevant literature will be discussed but not included in the calculations of sample cases. Two of these employ numerical methods that are much more complicated than the implementation of the small stage method algorithm described by Hundseid, et al. (2006). The third is a minor modification of Huntington's reference method. The calculation methods are listed in Table 3.

Comparing 12 polytropic head calculations based upon input from example cases available in the open technical literature yields trends that can assist an analyst in grasping the concepts and demonstrating the abilities of each method to perform accurate calculations under various conditions. Some of the head calculation results found in reference sources for inputs are typically based upon less than fully defined calculation techniques and the equations of state employed are not always documented. Thus, the Small Stage 100 step numerical method will be used as a basis for comparison of other methods in this paper. Since all methods are models with various underlying assumptions, the use of one method as a reference means the reported errors for other methods are in reality deviations from the reference result. A highly accurate, reference quality, equation of state methodology from a single source is applied to each example for consistency.

Table 3: Centrifugal Compressor Polytropic Performance Methods

Method Type	Origin	Description	Characteristics	Year
End Point	Schultz	2 End Points with correction factor	Constant polytropic exponent	1962
	Mallen and Saville	2 End Points	Simple equation	1977
	Sandberg and Colby	2 End Points with modified correction factor	Constant polytropic exponent	2013
	Schultz XY (2&3 Point)	Both End and Mid-Point methods with correction factor, averaged polytropic exponent	Constant polytropic exponent	1962
	Huntington 3 Point	End and Mid Points (3 points)	Z function of pressure only, iterative	1985
Stepped Numerical	Huntington Reference	Numerical Integration 20, 50, 350 Steps	Averaged volume across each step, nested iterations	1985
	Small Stage (Algorithm by Hundseid et al.)	Numerical Technique 20, 50, 100 Steps	Closest to true polytropic, iterative	2006
	Sandberg and Colby Reference	Numerical Integration 20 Steps; Uses Pv^n = Constant within each step	Iterate step temperature to match efficiency and check final temperature, nested iterations	2013
	Nathoo and Gottenberg*	Numerical Integration	Rearranged Schultz equations, iterative	1983
	Oldrich*	Numerical Integration (3 methods depending on inputs)	Rearranged Schultz equations, iterative	2010
	Wettstein*	Numerical Integration (a modified Huntington Reference Method)	Averaged temperature across each step, iterative	2014

* Not included in calculated examples.

THERMODYNAMIC CONCEPTS

Compressing a fluid requires energy input, however, unavoidable losses in that process mean more energy is required than is usefully transferred into the fluid. Some compressors require more energy input than others to achieve the same discharge pressure and consequently would have lower efficiency and higher discharge temperature. The laws of thermodynamics can be employed as an accounting procedure to evaluate efficiency of energy transfer processes. When determining the state point of a fluid, it is common to discuss properties such as pressure (P), temperature (T), density (ρ) (= 1/specific volume, v), and fluid composition. Enthalpy (H) and entropy (S) are two other state properties that are important to determining efficiency in a compression process. Changes in the state properties between initial and final fluid states should be calculated along the compression path in between to determine efficiency accurately.

The PV Diagram

James Watt and John Southern invented the predecessor of today's pressure volume diagram in the 1790s as a measurement tool (Miller, 2011). It was referred to as an indicator diagram and was used to study efficiency improvements for reciprocating steam engines. A mechanical device traced a line on a moving card with a pencil attached to a pressure gauge. The card movement was directly related to swept volume in the cylinder. The area encompassed by the resulting curve could be related to work performed. Watt considered the methods and use of the diagram to be a trade secret. In the 1830s, Clapeyron employed the indicator diagram concept to explain the Carnot cycle thus solidifying its place in the thermodynamics discipline as a handy analysis tool. Burgh (1869) wrote a comprehensive (at the time) book on indicator diagrams stating his inspiration was the fact that:

> *"A very large proportion of the young members of the engineering profession look at an indicator diagram as a mysterious production; and even supposing that they comprehend how it is formed, they do not understand the causes for the various forms of the figures."*

Watt's use of the PV diagram involved reciprocating steam engines that lent themselves to a fairly straight forward, continuous, analog measurement of the pressure and swept volume inside a cylinder throughout the extent of piston motion in real time. Today, this type of measurement is still used for performance measurements of reciprocating machinery but typically employs rapid digital sampling as the process occurs such that the resulting data sufficiently approaches an analog signal and represents reality without aliasing.

Measurements for centrifugal compressors on the other hand can only be made at discreet points before and after the compression process takes place. Unless a centrifugal compressor is used as a research project with many casing penetrations for expensive instrumentation, the measurement points are limited to piping segments outside the casing but near the suction and discharge flanges. If a control volume is considered to be everything internal to a compressor between the flanges, the goal is to determine what is happening inside using external measurements only. Drawing a PV diagram of the compression process must then rely upon mathematical modeling techniques and any accompanying assumptions. Matching these techniques to the physics of real gas behavior has been and continues to be a journey worthy of discussion. Clearly, a balance between required accuracy and complexity of implementation must be addressed, sometimes on an individual case by case basis. Complexity has become a moving target in that computing environment advances have made what was previously complex seem simple today.

Most engineers today have moved on to other mysterious subjects having conquered pressure volume diagrams in the first weeks of an elementary thermodynamics course. For an accurately drawn (calculated) PV diagram for compression, the area under the curve represents work performed while the curve itself represents the path. When specific volume (v) is used in the diagram, the work done on the fluid is determined on a per unit mass basis. Determining total work in a specific application would require a mass flow rate be known but efficiency can be calculated on a per unit mass basis.

Figure 1 illustrates a pressure vs. specific volume graph of a compression process for methane from a common suction state point to higher pressure along three paths with varying polytropic efficiencies of 100, 82, and 70 percent. In reality, the final thermodynamic state point (P, v, and T) for the 100% efficiency path cannot be reached due to losses along the compression path such as turbulence and friction within compressor passageways. Each path would reach the same final pressure at a larger specific volume since the final temperature is higher for lower efficiencies. The area beneath the 100 percent path represents the minimum amount of work required for compression between the initial and final pressures. Centrifugal compressor performance analysis is usually based upon a polytropic path with constant efficiency. A polytropic efficiency of 100% would make a polytropic path correspond to an isentropic

path since there is no increase in entropy. An isentropic process is defined as following a reversible adiabatic path (lossless). As polytropic efficiency decreases, the divergence of the paths increases illustrating more work is required at reduced efficiencies since the areas under the lower efficiency curves are greater. The path model used to create the curves in Figure 1 is based upon assumptions contained in ideal gas theory. Potential issues of using this path are discussed below, however, for methane at the pressures and temperatures shown in the graph, the path yields acceptable results. Noted on the graph is the relative area under each curve and required power differences as percentages of the 100% efficiency curve (assuming a mass flow rate of 1000 lbm/min). The area differences seem small compared to the power differences. The area differences are a measure of the required head increases (useful work) to reach the discharge pressure while the relative power differences are a measure of the enthalpy increases (total expended work) between suction and discharge which are impacted by the higher discharge temperatures.

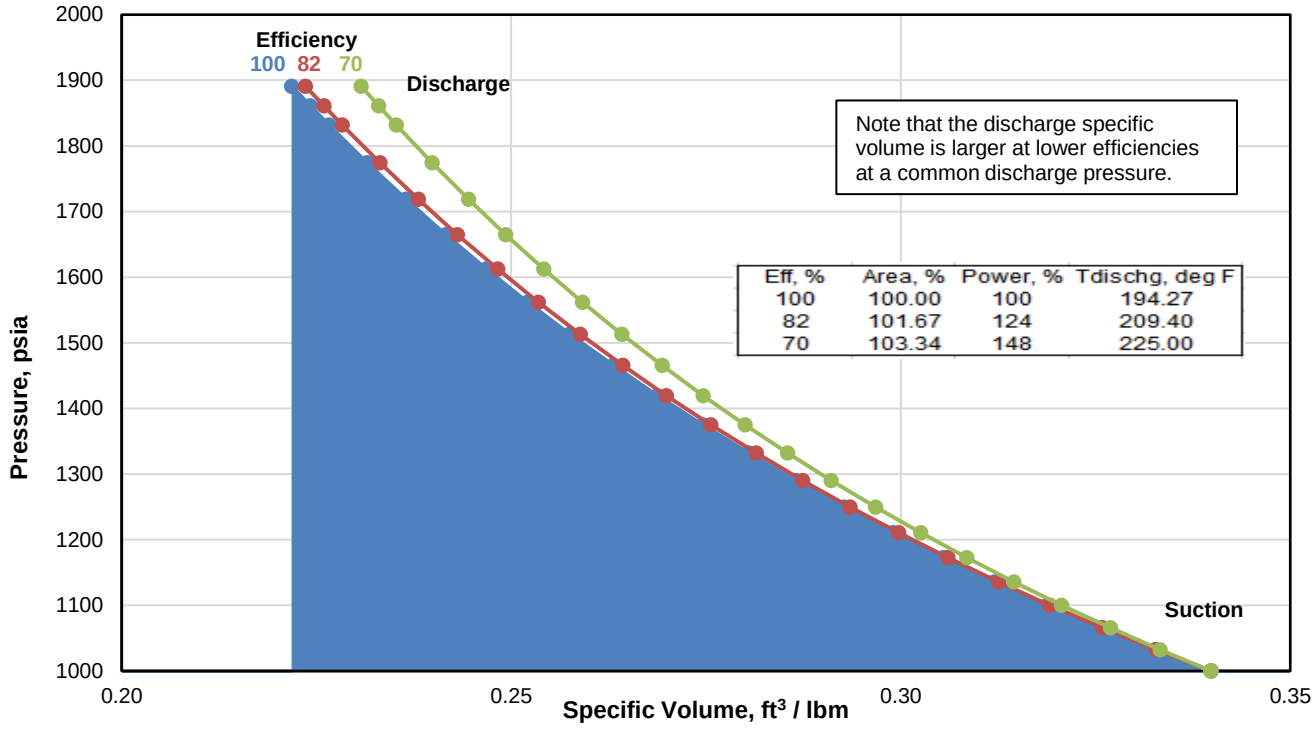

Figure 1: Compression Paths for Various Efficiencies Using PV^n = Constant

Power Test Code and Efficiency

Polytropic efficiency is typically defined as shown in Equation (1).

$$Polytropic\ Efficiency = \eta_{poly} = \frac{Input\ Work}{Enthalpy\ Change} = \frac{Head_{poly}}{\Delta H} = \frac{\int_{P_S}^{P_D} VdP}{H_D - H_S} \quad (1)$$

Schultz (1962) started his analysis by showing the need to solve the integral in the numerator of Equation (1) to obtain the area under the curve of pressure vs. volume. To accomplish this by closed form integration requires an analytical path equation to relate pressure and volume. In defining polytropic compression, ASME PTC 10 (1997), section 2.6.3 states "The polytropic process follows a path such that the polytropic exponent is constant during the process." This implies Equation (2) which is the starting basis for developing two common polytropic head equations (Equations (3) and (4)) as found in many literary reference resources. In this model, the exponent in Equation (2), n, is held constant throughout the compression path when in reality n varies from suction to discharge. The model can yield acceptable results in some cases if the variation of n is small. Equation (2) has its origins in perfect/ideal gas analysis

but has been commonly applied when analyzing real gases. Equation (5) defines the polytropic exponent, n, used in Equations (3) and (4) and is based upon the end points of the compression process.

$$Path\ Equation = PV^n = Constant \tag{2}$$

$$Polytropic\ Head = Head_{poly} = \left(\frac{n}{n-1}\right)[P_D V_D - P_S V_S] \tag{3}$$

$$Polytropic\ Head = Head_{poly} = \left(\frac{n}{n-1}\right)\left(\frac{R_0\, T_S\, Z_S}{MW}\right)\left[\left(\frac{P_D}{P_S}\right)^{((n-1)/n)} - 1\right] \tag{4}$$

$$Polytropic\ Exponent = n = \frac{LN\left(\frac{P_D}{P_S}\right)}{LN\left(\frac{V_S}{V_D}\right)} \tag{5}$$

Schultz also provided an alternate method to determine the polytropic exponent at a single point using Equations (6), (7), (8), and (9). Since the value of n varies along the compression path, being able to calculate n at several locations provided a set of values that could be averaged. Schultz showed the improvement that could be achieved with this method in an example.

$$Compressibility\ Function\ X = \frac{T}{V}\left(\frac{\partial V}{\partial T}\right)_P - 1 = T(volume\ expansivity) - 1 \tag{6}$$

$$Compressibility\ Function\ Y = -\frac{P}{V}\left(\frac{\partial V}{\partial P}\right)_T = P(isothermal\ compressibility) \tag{7}$$

$$Polytropic\ Temperature\ Exponent\ m = \frac{Z \times R}{C_P}\left(\frac{1}{\eta_{Poly}} + X\right) \tag{8}$$

$$Polytropic\ Volume\ Exponent\ n = \frac{1}{Y - m(1+X)} \tag{9}$$

$$Polytropic\ Head\ Factor = f = \frac{H_{Disen} - H_S}{\left(\frac{n_{isen}}{n_{isen}-1}\right)(P_D V_{Disen} - P_S V_S)} \tag{10}$$

Hundseid, et al. (2006), pointed out that Equations (3) and (4) would only yield the same results if Equation (5) was used to determine n. Schultz multiplied Equations (3) or (4) by a polytropic head factor, f, (Equation (10)), to provide a better match between model and measurement. To avoid distraction from the focus of this paper the reader is directed to a brief development of the two forms of the head equation in an appendix of Sandberg and Colby (2013) and additional relevant discussion can be found in Hundseid, et al. (2006), and Girdhar (2008).

It is interesting to note that an earlier version of ASME PTC 10 (1965) Section 2.31 described polytropic compression as "…a path such that, between any two points on the path, the ratio of reversible work input to the enthalpy rise is constant." This corresponds to Equation (1) and seems to embody the more fundamental definition mentioned by Schultz (1962) in his original development. Equation (11) is a stepwise restatement of Equation (1) that is used in some of the numerical integration methods to be discussed below. However, both ASME definitions quoted above have led to the same head Equations (3) and (4) due to assumptions made in their formulation. Thus two requirements have been imposed on centrifugal compressor polytropic performance analysis to conform to the current test code, constant efficiency and constant polytropic exponent. The former is required to solve the problem at hand but does not impact accuracy of a flange to flange analysis. The latter has been employed to make solutions easier to calculate based upon

closed form integration but potentially introduces significant errors. The errors that can be introduced by Equation (2) when applying Equations (4) and (5) (the ASME methods) can be reduced to insignificant values by applying Equation (11) instead.

$$Restatement\ of\ Equation\ (1) \qquad \eta_{poly} dH = VdP \qquad \text{or} \qquad \eta_{Poly} = {}^{VdP}/_{dH} \tag{11}$$

Origins of Polytropic Change of State

The origins of the ASME PTC 10 (1965) definition of polytropic compression were outlined by Wettstein (2014). He traced the concept of *polytropic change of state* back to books by Zeuner (1905) and Stodola (1910). Zeuner's 1906 book was a fifth edition and was translated from German into English by J. F. Klein (Zeuner, 1906). His first edition book was originally published in 1859 (some resources list 1860) in German and was entitled *Main Features of the Mechanical Theory of Heat*. Zeuner described it as *"…a clear and connected presentation of results of the scattered work of different authors which had appeared up to that time…"*. According to the fifth edition preface, Zeuner issued revised editions (also in German) in 1866, 1877 (name changed to *Technical Thermodynamics*), and 1901. Zeuner's career culminated with him teaching at the Royal Saxon Polytechnicum in Dresden (now called the Technical University of Dresden). The students educated under him are referred to as being from the Dresden school of thermodynamics (Encyclopedia of Human Thermodynamics, Human Chemistry, and Human Physics, 2015).

The referenced 1906 version of Zeuner's book (fifth edition) contained a footnote claiming Zeuner suggested Equation (2) in 1866. Equations (2) and (3) above are actually shown on pages 152 and 154 of Zeuner's fifth edition. In the development leading up to Zeuner's equations he noted that the analysis is based upon constant values for specific heats C_p and C_v which defines a perfect gas model. Stodola came to a similar result as Zeuner over 40 years later and Dzung (1944) provided the oldest reference to polytropic efficiency that relates to the form of Equation (11) (Wettstein, 2014).

Equation (2) and the Fallacy of Reification

Origins and assumptions used in development of Equation (2) as described above are not always presented together. With the proliferation of information available via the internet, it is possible to find seemingly credible resources that describe Equation (2) as if it is a fundamental truth instead of a model used for convenience. Thus an abstraction (the model) has been treated as if it is real. Tarpey (2009) describes this error in the following quote.

> *"The fallacy of reification is committed over and over, even by statisticians, who believe a particular model represents the truth … instead of an approximation."*

There are circumstances involving analysis of real gases when Equation (2) provides an inferior model of a compression path that can lead to large errors. While this does not completely condemn Equation (2), it points out that the underlying assumptions must be understood and evaluated for each application.

The ASME Power Test Code 10 (1965) provided the turbomachinery industry a consistent method for evaluation of polytropic efficiency that fit the then current computing and equation of state environments. This paper sheds light on whether the code should be updated to allow the employment of additional techniques after 150 years of working within the limitations imposed by Equation (2).

It is typical in textbook development of equations employed to model fluid compression to begin with general thermodynamic relations and center the discussion around so called ideal gases. This then leads to an isentropic analysis via the first and second laws of thermodynamics with resulting equations of the same form as shown above but with an isentropic exponent k (in place of n) that is defined as the ratio of specific heats. The exponent, k, is sometimes considered constant, but in reality varies. Further development toward polytropic analysis then follows. Sometimes, these subjects are presented during explanations of closed cycles thanks to Clapeyron's pressure vs. volume diagram introduction to the thermodynamics discipline mentioned above. The current discussion is limited to only the compression portion of an open cycle. For basic thermodynamic developments of fluid state points, relations, and closed cycles the reader is referred to Turns (2006) or other similar textbooks.

Issues Introduced by a Constant Polytropic Exponent

Equation (5) for the polytropic exponent n is solely based upon the endpoints of the compression path and n is also assumed to be constant per the Power Test Code. This constant value assumption is required to allow direct integration of Equation (1) to obtain Equations (3) and (4). However, limiting the exponent to a constant value can lead to errors in polytropic head calculations. Sandberg and Colby (2013) quantified the variation in polytropic exponent for compression and illustrated the causes. In some of their example

cases, holding the exponent constant yielded only minor errors while in other cases the errors were significant. This paper broadly quantifies the potential errors using Schultz's and other methods for real fluids in many example cases and provides an alternative to consistently reduce errors.

To illustrate the compression process path as modeled by Equation (2), pressure vs. specific volume and temperature vs. entropy graphs have been created for methane, carbon dioxide, and nitrogen from compression example cases. Figure 2, Figure 4, and Figure 6 illustrate the pressure vs. volume characteristics. Each graph shows three compression paths related to varying polytropic efficiencies. The 100% polytropic efficiency (also isentropic) path on each Pv graph shows that path reaches the final discharge pressure at a lower temperature than the other two paths. The two lower efficiency paths reach the final temperature of the 100% path at much lower pressures. Since the final temperature of each path at the common discharge pressure increases with lower efficiency, the attendant final specific volume is seen to be greater. A flow of 1000 lbm/min was assumed for each case to be able to compare the required input gas power as tabulated in the figures. Again, the 100% efficiency path requires the lowest power in each case. The Schultz method embodied by Equations (4) and (5) was used to calculate the polytropic exponent and gas power while the curves were drawn using Equation (2) and an equation of state. The endpoints of these curves represent data points employed by the current power test code to generate centrifugal compressor performance results.

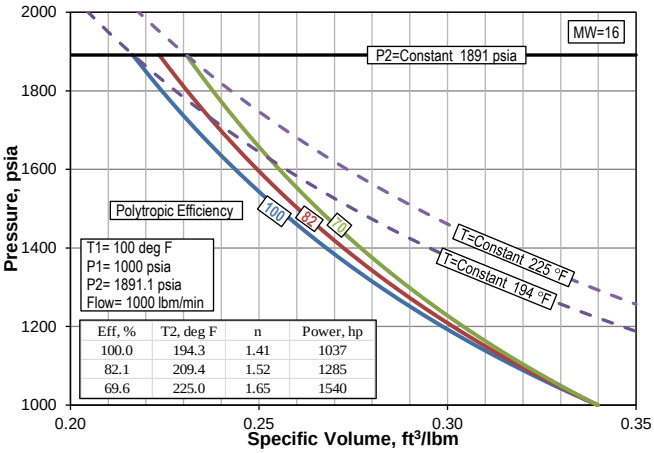

Figure 2: Methane Pv Diagram, PV^n = Constant

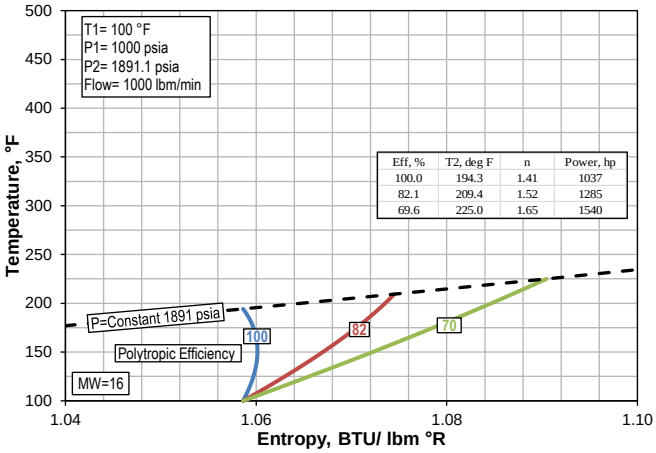

Figure 3: Methane TS Diagram, PV^n = Constant

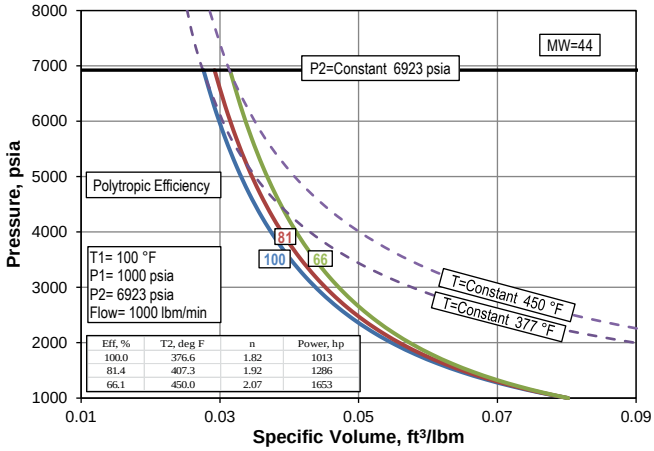

Figure 4: CO2 Pv Diagram, PV^n = Constant

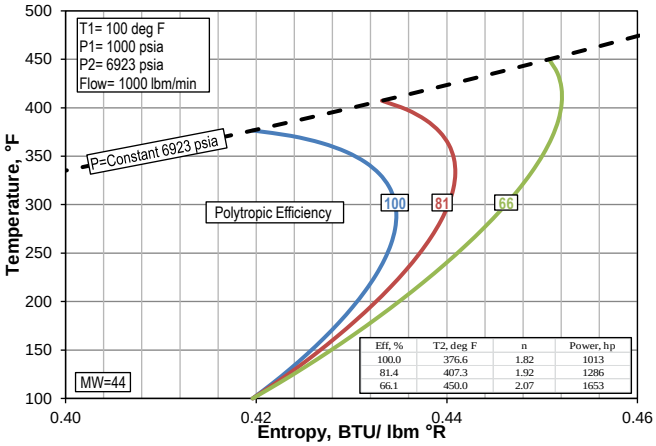

Figure 5: CO2 TS Diagram, PV^n = Constant

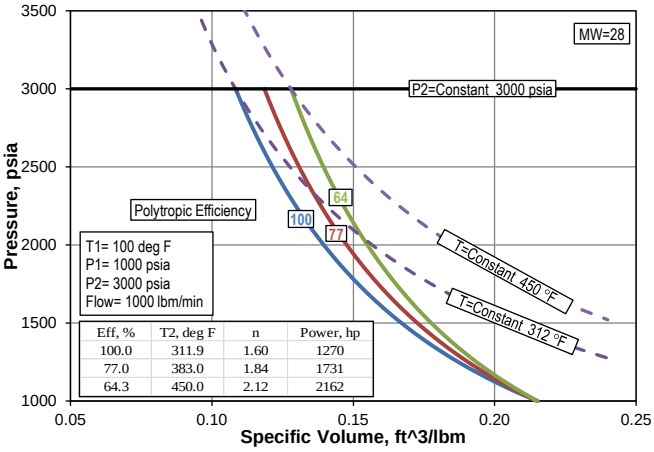

Figure 6: Nitrogen Pv Diagram, PV^n = Constant

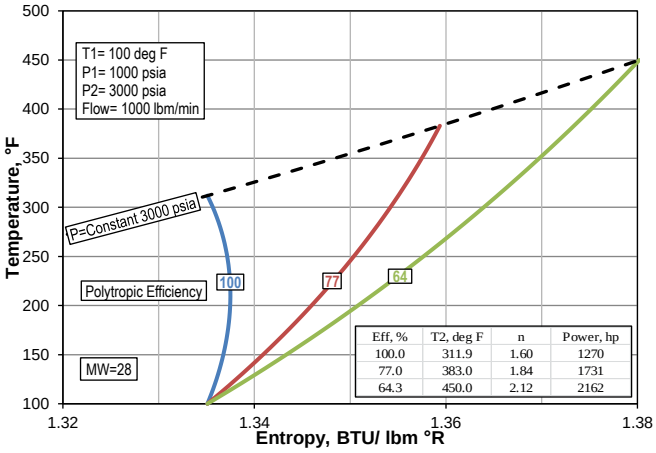

Figure 7: Nitrogen TS Diagram, PV^n = Constant

Figure 3, Figure 5, and Figure 7 illustrate the temperature vs. entropy characteristics for the same sample cases shown in Figure 2, Figure 4, and Figure 6. The 100% efficiency paths should be straight vertical lines in the graphs. However, some slight curvature is seen for methane and nitrogen while a large curvature is seen for carbon dioxide. This makes the other constant efficiency path curves for carbon dioxide suspect also. The three graphs have the same vertical axis scale and the same change in entropy scale of 0.06 Btu/lbm °R allowing direct comparison of the curve shapes on the three graphs. In Figure 5, the excursion of what should be a constant entropy, vertical line (100% efficiency) shows first an increase in entropy with pressure and then an equal decrease in entropy as pressure continues to increase through the compression process. In a strict sense, this is a violation of the laws of thermodynamics. In compressor performance analysis, as in many other engineering calculations, determining a result even though known laws seem to be violated is sometimes addressed by using *correction factors*. This was Schultz's approach. It falls to the analyst making the calculations to determine if the *corrected* result lies within an acceptably small error tolerance. However, that is not an easy judgement to make when real gas conditions exist.

Since the polytropic exponent for the Schultz method is based upon the compression path end points, it makes sense that the initial and final entropy for the 100% efficiency paths are equal, i.e., $(S_D - S_S) = 0$ in Figure 3, Figure 5, and Figure 7. Drawing the curve in between points S and D based upon the chosen path (Equation (2)) does not always yield favorable results. Schultz applied a correction factor to adjust the head calculations made with Equations (3) and (4) however, it does not always sufficiently account for the variation in polytropic exponent, n, from one end of the path to the other. Figure 8 illustrates an example of the variation of n from suction to discharge of a mixture of methane and CO2 (70/30%). The n value increases by about 52 % but is very nearly linear such that an average value provides an error of only -0.076 % using Schultz's XY end point method. Other examples listed below are seen to not be well suited for this method.

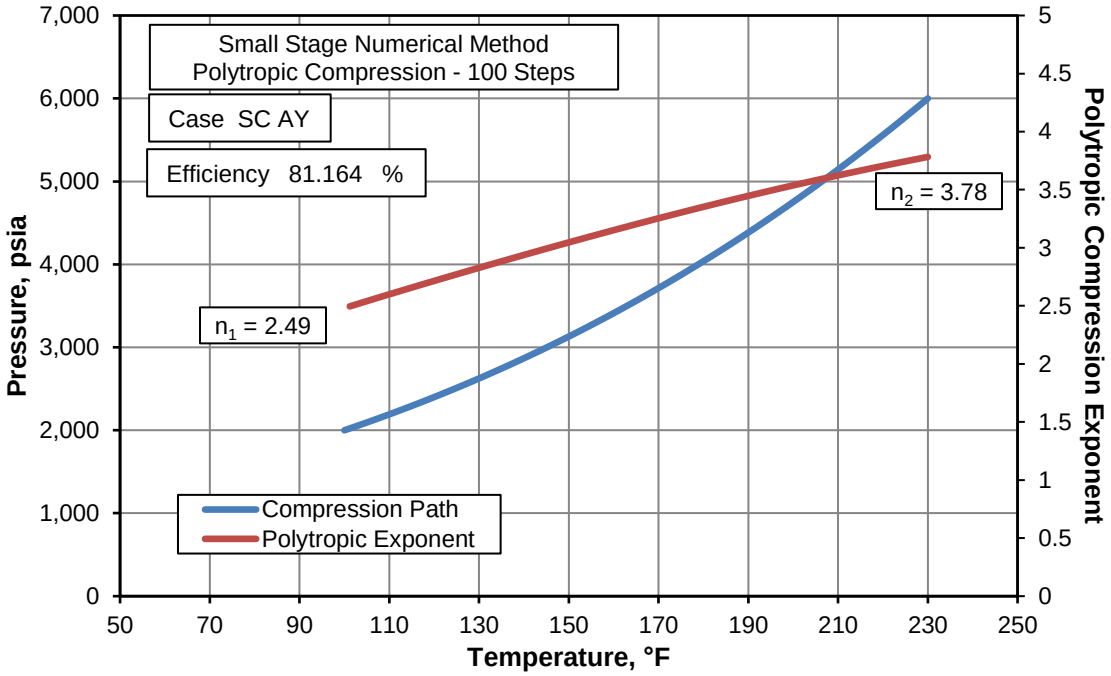

Figure 8: Variation of n for Methane/CO2 Mixture

The degree to which a gas mixture shows excessive differences between Schultz's calculation method results and reality when being compressed depends upon the mixture constituents, their relative volume percentages, and suction and discharge conditions. Alternative calculation methods exist that sufficiently reduce errors and thus do not require the same level of discernment of acceptability of results as Schultz's methods (Evans and Huble, 2017).

Enthalpy and Entropy

Enthalpy is a fairly well recognized concept in the subject of compressor efficiency calculations. While it cannot be directly determined in the ways pressure and temperature can be measured, within the culture of the thermodynamics discipline it is commonly discussed as if it could be. In other words, most analysts are familiar enough with the concept of enthalpy changes being related to energy expenditures to be at ease with it. However, entropy is less obviously present on the surface in classic Schultz style performance calculations since it is only needed in determining the correction factor. Some treatments of polytropic performance analysis omit the correction factor since it requires additional thermodynamic calculations and can be a number close to 1.0.

Mentioning entropy could raise connotations of complexity in an analyst's mind. The word was coined in 1865 by Clausius as described in the following quote by Klein (1989).

> *"It was not until 1865 that Clausius invented the word entropy as a suitable name for what he had been calling 'the transformational content of the body.' The new word made it possible to state the second law in the brief but portentous form: 'The entropy of the universe tends toward a maximum,' but Clausius did not view entropy as the basic concept for understanding that law."*

The stepped numerical methods described below in this paper will make critical use of quantitative measures of changes in entropy which today can be found by simple calls to an equation of state subroutine for known fluid state points. A qualitative understanding of entropy can take several directions. Alternate names for entropy and enthalpy have been suggested as Messy and Lazy respectively, as mentioned in the following quote.

> *"As students, we daily battle entropy and enthalpy. Entropy being the disorder in the world and enthalpy being energy expenditures. We, as human beings as in Nature, tend toward high entropy and low enthalpy…we're messy and lazy. (Write in the margins, 2013)."*

However, Lambert (2013) provided an excellent discussion on entropy strongly disagreeing with the above simple characterization with the following conclusion.

> *"The second law of thermodynamics says that energy of all kinds in our material world disperses or spreads out if it is not hindered from doing so. Entropy is the quantitative measure of that kind of spontaneous process: how much energy has flowed from being localized to becoming more widely spread out (at a specific temperature)."*

In the compression process, entropy is increased due to inefficiencies in the process of energy transfer from a moving mechanical device to a flowing fluid and is manifested by a measureable increase in discharge temperature above the theoretical isentropic discharge temperature. Fortunately for the gas compression industry, the thermodynamics discipline has developed theoretical relationship models between the various fluid state point variables and their derivatives (via equations of state) that allow entropy to be easily quantified. More specifically, entropy changes can be quantified as easily as enthalpy changes are quantified by today's equations of state. Thus, dealing with compression models involving entropy change can be addressed without an analyst having to gain a firm grasp of statistical thermodynamics where a broader understanding of entropy can be found. (Care must be taken to avoid comparing absolute values of entropy and enthalpy from different sources since the reference states for each may be different. However, changes in these quantities can be compared.)

Figure 9 illustrates a full stage compression process in an enthalpy vs. entropy diagram (also called a Mollier diagram). Lines of constant pressure are shown as black dashed and dotted lines while the vertical blue dashed line represents constant entropy between the suction point, P_1, and the discharge pressure line at point P_{2s}. The red line represents the constant polytropic efficiency compression path from point P_1 to point P_2 between the two constant pressure lines. Two broad classes of polytropic performance analysis methods have been labeled as end point methods and numerical methods. The end point methods use thermodynamic state point information at points P_1, P_{2s}, and P_2 and a constant polytropic exponent from Equation (5) in their calculations. The required path equation for the red line is provided by Equation (2). The isobars shown in Figure 9 diverge which gives rise to the fact that isentropic efficiency is less than polytropic efficiency for compression processes (Evans and Huble 2017).

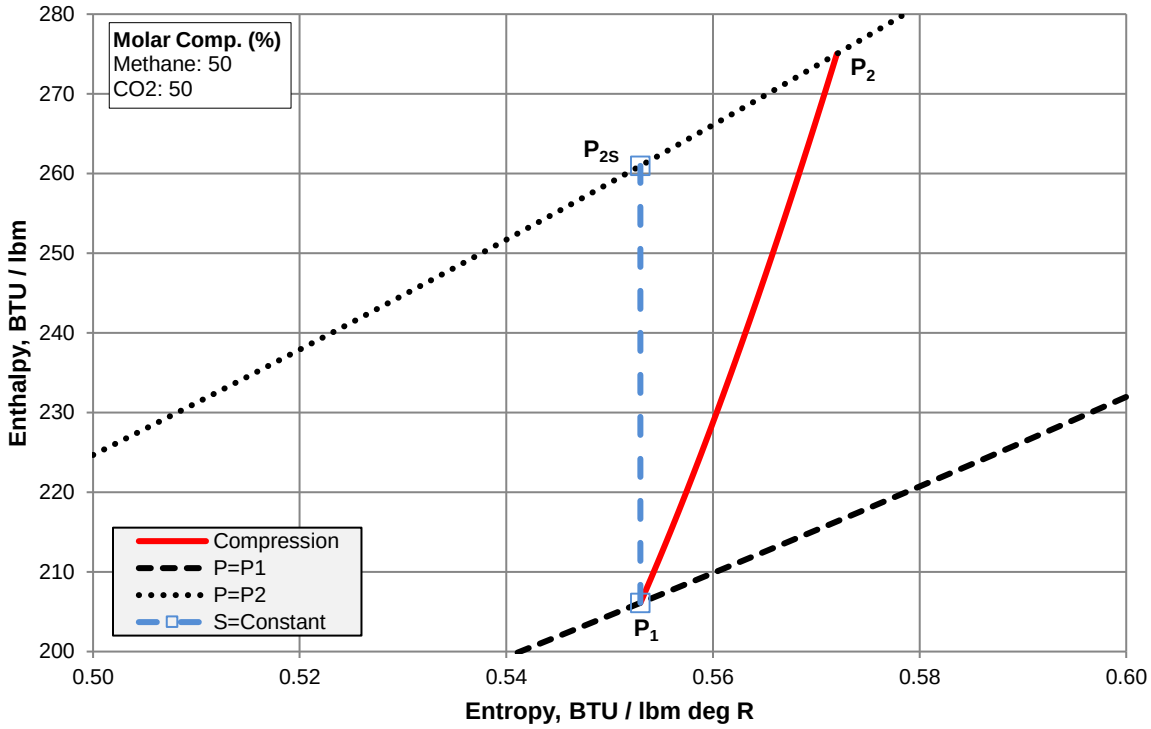

Figure 9: Full Stage Compression in the Mollier Diagram

Since the centrifugal compression process is generally represented by a well behaved, monotonically changing path, some numerical methods use Equation (11) as described in the next paragraph to calculate the path represented by the red line and resulting polytropic head.

Numerical Methods

If the line between points P_1 and P_2 in Figure 9 is broken into many small, constant efficiency, pressure step segments of a similar shape to the approximate triangle with vertices at P_1 P_{2s} P_2 of Figure 9, calculations can be made for each small step. Since efficiency has been held constant, the summation of calculated results for each step can be used to determine performance. Figure 10 shows two small successive steps within the compression process shown in Figure 9 for subpath pressures P_i, P_{i+1}, and P_{i+2}. Along the compression path, the first two pressures are connected by segment P_1-P_2 while the next two pressures are connected by segment P_2-P_3. Huntington's (1985) numerical method (discussed below) can be used for the summation of results for the individual segments via iterative techniques. These techniques calculate polytropic head and specific volume within each step by averaging initial and final step conditions similar to a mathematical quadrature (using a trapezoidal rule). Since the segments are small, the actual compression path is considered linearized within the step. Iteration of assumed efficiency is required to reach convergence for final boundary conditions or to approach convergence within a sufficiently small, acceptable tolerance. Sandberg and Colby (2013) used Equation (2) within each step as a path equation for a reference method and used similar summing techniques across all steps to get the overall result. A third numerical method is described below based upon the Hundseid, et al. (2006), algorithm and was implemented by Evans and Huble (2017) for many example cases.

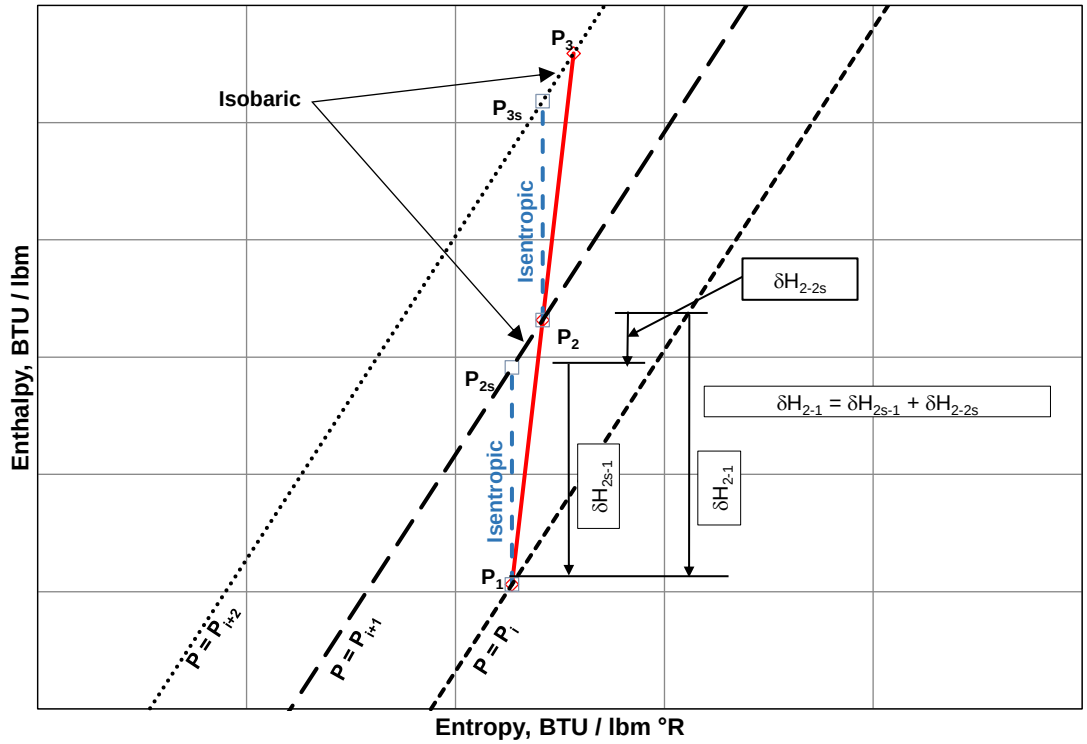

Figure 10: Small Stage Stepped Compression Concept

The Small Stage – Polytropic Compression

At this point it is useful to introduce an additional concept and form of the equation for determining polytropic efficiency. If the small pressure step segments described in Figure 10 are infinitesimal in size, each is referred to as the *small stage* (Cumpsty, 1989). Following the algorithm of Hundseid, et al. (2006), theoretically separating each pressure step into two parts, one of isentropic compression followed by the other, isobaric heat addition, assists in the discussion. For each small stage, the adiabatic, isentropic compression work (δH_{2S-1} or δH_{3S-2}) is represented by vertical blue dashed lines $P_{1\rightarrow 2s}$ or $P_{2\rightarrow 3s}$ in Figure 10. The isobaric heat addition is represented by a portion of the dashed black lines labeled $P_{2S\rightarrow 2}$ or $P_{3S\rightarrow 3}$. The enthalpy increases associated with segments $P_{2S\rightarrow 2}$ or $P_{3S\rightarrow 3}$ are called *heating losses*. The actual work in a single polytropic segment, δH_i, is represented by the vertical enthalpy rise associated with the solid red lines $P_{1\rightarrow 2}$ or $P_{2\rightarrow 3}$. The small stage efficiency for each step is the minimum compression work required divided by the actual work expended which is the ratio shown in Equation (12). Since the efficiency is constant for each small compression step, the results can be summed to get the full stage results by Equation (13). Comparing Equation (13) to Equation (1) shows the numerator of Equation (1) has been replaced by the summation of the isentropic enthalpy changes for all of the small stage steps. Thus, calculating a linearized average volume for each step as is performed in other numerical methods is not required. The denominator of Equation (13) is numerically equal to the denominator of Equation (1).

$$\eta_{Poly_i} = \delta H_{isen_i} \;/\; \delta H_i \qquad \eta_{Poly_i} = constant \tag{12}$$

$$\eta_{Poly} = \sum_{i=1}^{\infty} \delta H_{isen_i} \;/\; \sum_{i=1}^{\infty} \delta H_i \qquad \eta_{Poly} = \eta_{Poly_i} = constant \tag{13}$$

$$PR_i = \left({}^{P_D}/_{P_S}\right)^{1/j} \qquad \text{(must use large enough value for j for PR to be } \approx 1) \tag{14}$$

For this small stage method summation to achieve acceptable results requires the pressure ratio of each step to be relatively close to 1.0. Equation (14) can be used to determine a constant pressure ratio, PR, between each pressure step based upon the total number of steps, j. Using Equations (12) and (13) in a numerical summation is simpler than using Equation (11) since it requires fewer iterations and eliminates averaging of thermodynamic properties. The step pressure ratio must be kept near 1.0 to avoid excessive influence of the diverging isobars is an HS diagram.

Either approach to the numerical methods can yield reasonable results when used with an appropriate equation of state.

In reality, computerized implementation of the numerical techniques cannot use an infinite number of steps, but a sufficient number of steps, j, can be employed to achieve an acceptably small tolerance between successive iterative calculations. The difference between results for increasing numbers of steps asymptotically approaches zero as shown in Figure 11 for the small stage method. For an arbitrarily chosen maximum acceptable error tolerance of 0.1 % of total head, a minimum of 30 equal ratio (PR= 1.055), small pressure steps are required for this particular chosen fluid mixture and suction and discharge conditions. Other fluids and conditions might require fewer or more steps to achieve the same arbitrary tolerance. The small stage calculation method has been called the most accurate by both Hundseid, et al. (2006), and Taher (2014). For the example cases reported below, the *small stage method* with 100 steps was chosen as a basis for comparison of the other calculation methods. With a calculation approach employing Equations (12) and (13) and a well-qualified equation of state, the fourth issue listed in Table 1, polytropic performance calculation method accuracy, can be addressed.

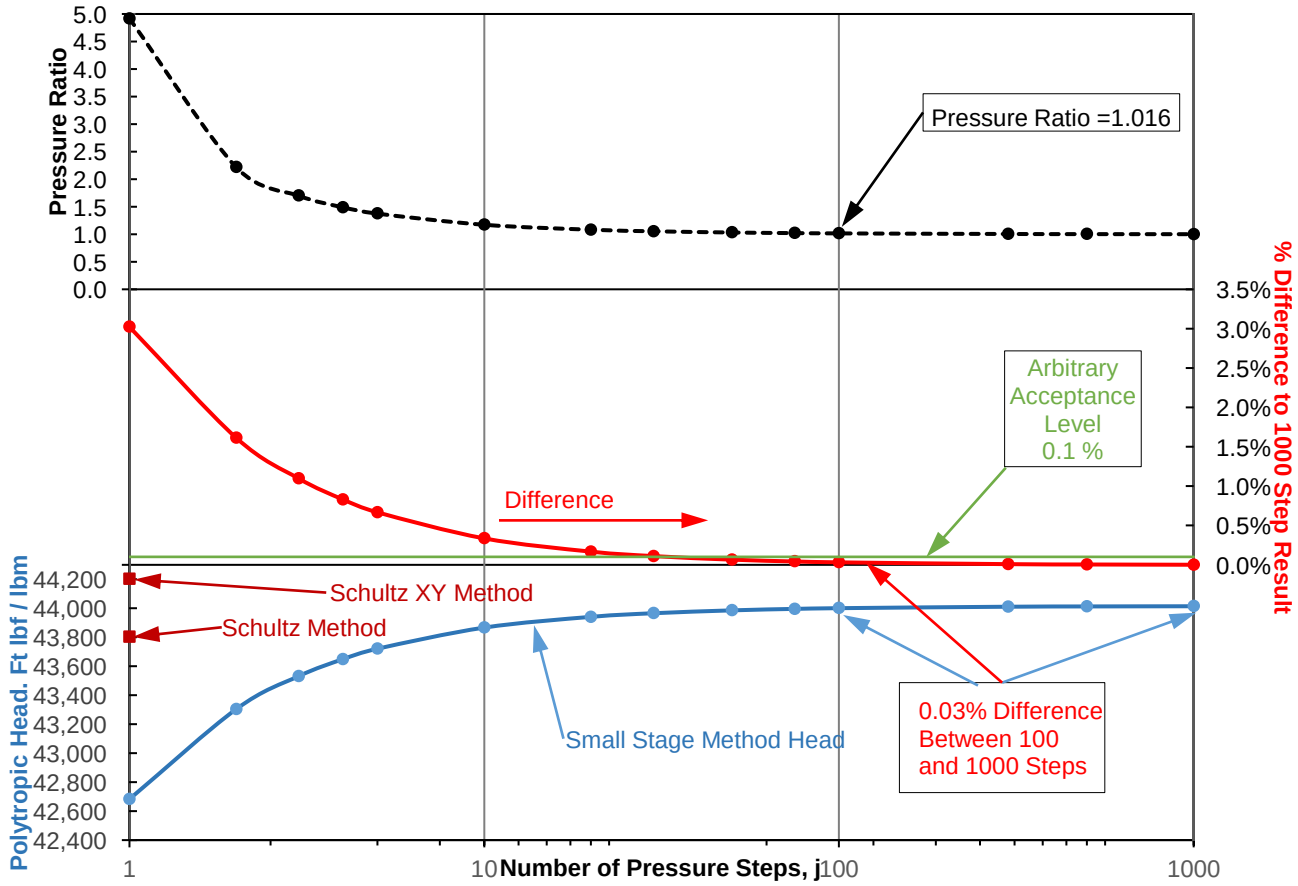

Figure 11: Polytropic Head vs. Number of Pressure Steps

Schultz provided the real gas, constant polytropic exponent method and ASME adopted it in an era when computing power was expensive and access was limited. Additionally, access to and use of equations of state was progressing but suffered from similar computing limitations and a lack of sufficient fluid property measurements (PvTx, etc.) for many pure fluids and mixtures at various state points for comparison. Most thermodynamic property calculations performed when Schultz wrote his paper employed interpolation of tabulated data by hand, Mollier diagrams for pure fluids, and generalized compressibility charts after using a mixing rule for various constituents. As operating pressures increased thereby pushing fluids into the dense phase region, other analysts followed in Schultz's footsteps using compression endpoint states for calculations in an effort to improve agreement between measurements and calculations. The proposed techniques involved replacing the head equation, replacing the correction factor, and/or adding midpoint calculation methods. Several analysts checked their work with stepped numerical integration of a form derived from Equation (11) and stated that was the most accurate method but stopped short of suggesting it be used on a full time basis. As computing access and power evolved, enormous strides were made in calculation precision and speed. Also, fluid property measurements flourished with an attendant improvement in equations of state. The two bottlenecks of computing power and equations of state are no longer a deterrent to accurately determining polytropic head for a centrifugal compressor. However, significant errors can still be made based upon the selected method for polytropic head calculation and uncertainty in composition of the fluid mixture being analyzed. This paper aims to address calculation methods such that an analyst can easily select a method that will provide results within the required accuracy.

FLUID PROPERTIES VIA EQUATIONS OF STATE

Measureable fluid properties such as the pressure, temperature, and volume (among others) can be used to define a fluid's thermodynamic state. The compression process is employed to achieve a desired change of state of the fluid to a higher pressure and inherently, a higher temperature. The thermodynamic behavior of the fluid as it is being compressed is a necessary input to performance analysis. Today, we typically use mathematical models called equations of state (EOS) to estimate a fluid's properties at necessary state points. Technical literature abounds with various versions of equations of state, both general and specific, that can be employed to investigate and model fluid behavior. How well an EOS duplicates the measured properties of a fluid within a particular range of interest directly impacts centrifugal compressor performance analysis results.

While this is not the main subject of this tutorial, fluid properties are an important part of performance calculations for centrifugal compressors. The discussion below is aimed at providing a starting point to develop the necessary background an analyst needs to navigate through a selection of several equations of state that have become the workhorses of the compressor industry. It is by no means exhaustive, but perhaps it will be enlightening and encourage further study as it simply scratches the surface of the subject.

Ideal vs. Real Gas

Some characteristics of perfect, ideal, and real gases were previously defined in Table 2 above. In 1834, Clapeyron combined the findings of several early fluid property researchers and contributed what became known as the perfect or ideal gas equation of state, shown in Equation (15). In 1822, Cagniard de la Tour listened to the sounds of a flint ball rolling down a closed cannon barrel containing fluids at different temperatures. What he discovered was the critical state of a fluid where liquid and gaseous phases cease to exist separately. Fluid properties at an individual state point can be expressed as reduced properties by dividing them by the corresponding critical point property values as shown in Equations (16), (17), and (18) (Walas, 1985).

$$Ideal\ Gas\ EOS \rightarrow PV = RT \tag{15}$$

$$Reduced\ Pressure = P_r = {}^{P}/_{P_c} \tag{16}$$

$$Reduced\ Temperature = T_r = {}^{T}/_{T_c} \tag{17}$$

$$Reduced\ Volume = V_r = {}^{V}/_{V_c} \tag{18}$$

The current ASME Power Test Code (1997) recognizes that real gases can sometimes be treated as ideal gases with acceptable results. For some gases at low pressures and moderate to high temperatures, the ideal gas equation might provide a useful relationship, but it can not represent all thermodynamic states of a fluid, specifically any liquid or vapor (two phase) states. Gases that depart from ideal behavior are referred to as real gases and can be represented by an equation that introduces a compressibility factor, Z, as shown in Equation (19). The following discussion centers around terms added to or modified within a real gas EOS in an effort to improve the relationships between measured and model estimated values of multiple thermodynamic properties. Equations defining Z can have multiple terms and the real gas EOS can be cast into other forms to solve for P or Z.

$$Real\ Gas\ EOS \rightarrow PV = ZRT \tag{19}$$

Fluid Mixtures

Thermodynamic properties of fluid mixtures are usually obtained by calculating properties for each pure component and then combining the respective values with prescribed mixing rules. Early mixing rules were based upon molar volume percentages of each component. This type of rule is still used today to determine the molar mass of a mixture but has typically been replaced by more sophisticated rules for other properties. Many times, these rules use binary interaction parameters based upon experimental measurements. For purposes of this discussion it is sufficient to indicate that this subject is very relevant to accuracy and can be as simple or complicated as are pure fluid equations of state. Fluids are very diverse and just as one EOS may not fit all fluids, mixing rules may be varied to deal with the diversity. The reader is encouraged to explore this subject to get a flavor for various methodologies.

Molecular Forces

Some molecular level forces between molecules of a fluid have been modeled as a combination of repulsive and attractive forces. These can be thought of as interactions between electrons and nuclei of one molecule and those of another molecule (negative and positive electrical interactions). The closer the molecules are to each other, the higher the repulsive forces which would tend to lead to expansion. The attractive forces would tend to contribute to compression. The repulsive forces dominate when molecules are very close and almost touching. The attractive forces are dominant at somewhat higher separation distances but decrease as molecules get further and further apart. These forces are impacted by operating conditions and can play a role in whether or not a gas acts in an ideal manner or must be treated as a real gas.

Figure 12 qualitatively illustrates models of the relative potential energies related to the intermolecular forces described above. For various fluids, the basic curve shapes could be consistent but would likely lie in different areas on the graph. The two curves on the left side of the figure show the repulsive potential is positive and the attractive potential is negative. Forces would be related to the slopes of the curves such that as the separation distance increases, both forces decrease (flatter slopes) with the repulsive term falling much faster than the attractive term. The slope of the repulsive curve is always negative while that for the attractive curve is always positive. The largest potential is seen to be as the repulsive curve approaches the left axis meaning molecules are about to touch. The net combined potential curve is shown on the right side of the figure. Molecule shapes (polar vs. non-polar, etc.) can impact the characteristics of the potential curves. The separation distances over which these forces are significant is on the order of several molecular diameters. There are other models of repulsive and attractive potentials that can be found in the literature. The purpose of the above limited discussion is to illustrate that terms in some equations of state discussed below are related to physical phenomena.

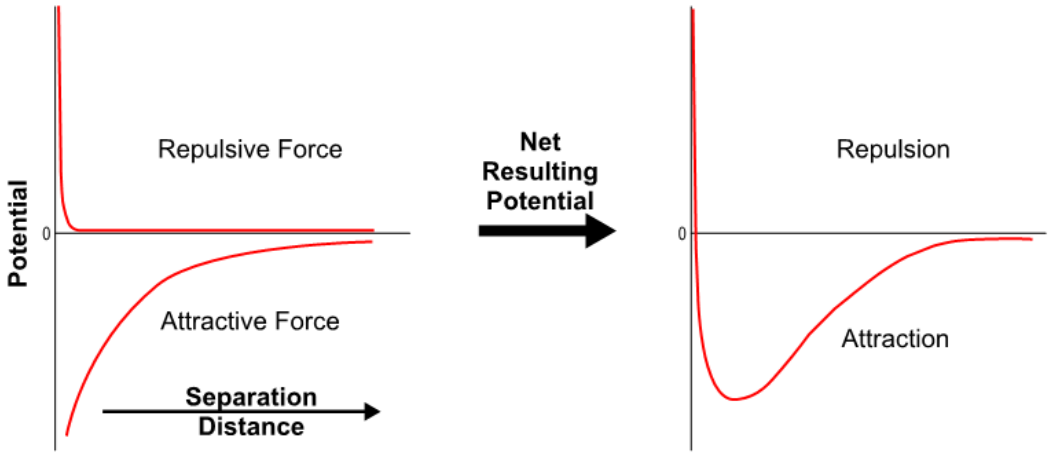

Figure 12: Molecular Potential Energy Model

The Beginning: van der Waals' EOS

In 1873, van der Waals published a dissertation (van der Waals, 1873) proposing a new EOS for real gases as shown below in Equation (20). It has been said that the original version of this reference must be "*the most cited and least read of any thesis in physical science.*" In 1910, van der Waals received the Nobel Prize for Physics "*for his work on the equation of state for gases and liquids.*" In the lecture he presented when the prize was awarded, (van der Waals, 1910) he indicated that his motivation was that he thought that gases and liquids (fluids) must be different regions of a continuum based upon his study of prior work by Clausius which claimed *"gas consists of material points which move at a high velocity."* In other words, the molecular phenomena that apply to gases, apply to liquids also, only differing quantitatively. van der Waals' equation provided the beginning of a long string of equations of state that is still expanding today, each offering some refinement, expansion, replacement, and/or special region of application. Walas (1985) provides extensive discussion and two detailed tables illustrating some aspects of the early history of equations of state.

$$van\ der\ Waals' EOS \rightarrow P = \frac{RT}{V-b} - \frac{a}{V^2} \tag{20}$$

In Equation (20), a and b are constants with different values for each pure gas. For the terms on the right hand side, the one containing "a" is intended to account for intermolecular attractive forces while the term containing "b" accounts for the fact that the molecules actually occupy a finite portion of the volume themselves. This *excluded volum*e term in van der Waals EOS, (V-b), is sometimes thought of as being related to repulsive forces between molecules. Values for constants a and b for each pure gas can be determined based upon properties at the critical point of each gas. The development of Equation (20) is shown below in Equations (21), (22), (23).

$$(p + \Delta p)(V - \Delta V) = RT \tag{21}$$

$$\left(p + \frac{a}{V^2}\right)(V - b) = RT \tag{22}$$

$$p = \frac{RT}{V-b} - \frac{a}{V^2} \tag{23}$$

The concept to grasp is that in van der Waals' *real* EOS model of fluid behavior, the ideal gas pressure is modified by an excluded volume term, (V-b), and a molecular attractive force term (a/V^2). At large volumes, b becomes negligible compared to V and the (a/V^2) term becomes very small such that in the limit, the result is similar to the ideal gas EOS. Large volumes are indicative of low pressure and high temperatures where the ideal gas EOS seems to work.

The van der Waals EOS provided qualitative results in line with observed phenomena such as two phase equilibrium regions and liquids as well as gases. However, quantitatively it was less useful and even van der Waals himself did not expect it to be highly numerically accurate. It gave rise to what today are called cubic equations of state, i.e., the solution can have three roots. One problem with the van der Waals EOS is that the compressibility, Z, at the critical point is predicted to be the same for any gas ($Z_c = 0.375$) which illustrates some of its quantitative limitations since the experimental range for Z_c for various gases has been documented to be approximately from 0.23 to 0.31. The cubic EOS discussion below will show that many have retained the basic form of van der Waals' EOS while improving on the numerical accuracy of matching measured data by using variable coefficients.

Using van der Waals' EOS, an isotherm drawn on a phase diagram of a fluid that passes through the critical volume has first and second derivatives that are equal to zero. This information can be used to determine the constants a and b in terms of critical properties as shown in Equations (24) and (25) below. This allows the van der Waals EOS to be cast in terms of reduced properties thus eliminating a and b. The result is Equation (26). This reduced form led van der Waals to the principal of corresponding states which is discussed below.

$$a = \frac{27R^2T_c^2}{64P_c} \tag{24}$$

$$b = \frac{RT_c}{8P_c} \tag{25}$$

$$P_r = \frac{8T_r}{3V_r - 1} - \frac{3}{V_r^2} \tag{26}$$

Corresponding States

The principal of corresponding states provides that fluids that have equal reduced pressures and reduced temperatures have equal reduced volumes and equal compressibility factors, Z. Thus, they would be predicted to deviate from ideal gas behavior in a similar manner. The Schultz compressibility functions X and Y shown in Equations (6) and (7) above allowed use of the principal of corresponding states to determine the polytropic volume and temperature exponents, n and m, if sufficient test fluid thermodynamic property data was not available.

This principal can be illustrated in Figure 13 which shows the compressibility, Z, of several fluids as a function of reduced pressure and reduced temperature. The original version of this type of graph was generated from actual measured data for each included fluid. The data shown in Figure 13 has been developed from reference quality EOS for each fluid. Note that at low reduced pressures, the data points for all fluids shown are tightly grouped but become more spread out at higher reduced pressures and temperatures. This indicates that the corresponding states principal has its own limitations. The data points for methane are connected by the blue lines to help illustrate the trends. Note that the critical points are not at the minimum values. Using more points in the minimum value region would likely show a smoother transition between negative and positive sloped regions. Also note the crossover of constant reduced temperature curves at higher reduced pressures.

Pitzer (1955) expanded the corresponding states theory by including the acentric factor, ω, which describes the deviation of the reduced vapor pressure of a fluid from that of a simple molecule. Equation (27) shows the definition of the acentric factor. Using three parameters for correlation (P_r, T_r, ω) provided better corresponding states results for fluids containing non-spherical molecules.

$$Pitzer's\ Acentric\ Factor \rightarrow \omega = -log_{10}\left(\frac{P_{sat}}{P_c}\right) - 1 \qquad \text{at a reduced temperature of 0.7} \qquad (27)$$

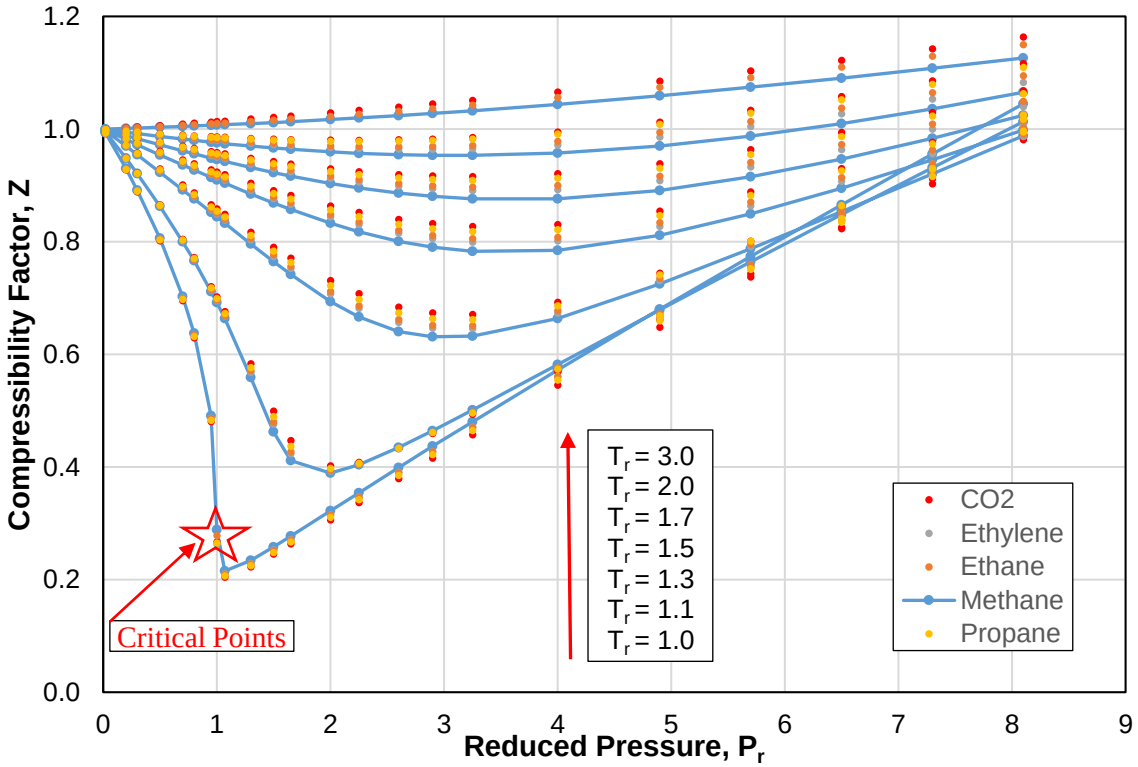

Figure 13: Illustration of Corresponding States

Virial Equation of State

The constants a and b in van der Waals' EOS became the subject of investigations attempting to cast them not as constants but as empirical functions of temperature and volume to improve quantitative results. Kamerlingh Onnes (1902) landmark paper described these efforts as "*without obtaining good agreement with the observations over the whole range of the equation of state*." He wrote "*Hence it appeared to me more and more desirable to combine systematically the entire experimental material on the isothermals of gases and liquids as independently as possible from theoretical considerations and to express them by series*."

Equation (28) shows the form of Onnes' virial equation of state. Pressure is shown to be a function of temperature and density and is the sum of an infinite polynomial series of density multiplied by temperature dependent coefficients B, C, D, etc., which are referred to as the second, third, and fourth virial coefficients. When the equation was introduced, all calculations were done by hand which made determining higher order virial coefficients impossible. Typically, the terms containing density to the third power and higher are truncated. This limited the ability of the equation to produce results for all fluid phases, but it could handle gas states better than van der Waals style cubic EOS. The term virial, when used as an adjective to describe an equation of state, is defined as pertaining to interactive forces between molecules. Through statistical thermodynamics, the virial coefficients, B and C, have been related to interactions between pairs and triplets of molecules.

$$Virial\ EOS \quad Z(T,\rho) = \frac{p(T,\rho)}{\rho RT} = 1 + B(T)\rho + C(T)\rho^2 + D(T)\rho^3 + \ldots \tag{28}$$

Benedict, et al. (1940), provided a modification of Onnes' virial equation by adding an exponential term as shown in Equation (29). The exponential term was intended to be an adjustment to account for the truncated higher order terms of the virial EOS. This has become known as the BWR EOS. A version was added in 1942 to allow calculations for fluid mixtures (Benedict, et al.,1942). Other researchers have modified the BWR EOS to provide improvements for specific fluids and phase regions. (Span, 2000; Walas, 1985)

$$BWR\ EOS \quad Z(T,\rho) = \frac{p(T,\rho)}{\rho RT} = 1 + \sum_{i=1}^{6} n_i T^{t_i} \rho^{d_i} + \sum_{i=7}^{8} n_i T^{t_i} \rho^{d_i} \exp\left(-\left(\frac{\rho}{\rho_r}\right)^2\right) \tag{29}$$

The BWR style EOS requires the determination of many coefficients for each fluid. In one form or another, it has become widely used in the calculation of thermodynamic properties for the hydrocarbon processing industry. Walas (1985) provides further background information and a table describing the coefficients for virial EOS including the BWR version. Each analyst's implementation likely uses customized coefficients.

Cubic Equations of State

Of the many van der Waals' style equations of state that have been put forward, three have become well known due to their ability to provide results accurate enough to have been incorporated into many compressor investigations. These are Redlich Kwong (1949), Soave Redlich Kwong (1972), and Peng Robinson (1976), and are referred to as RK, SRK, and PR respectively. Each of these modified the attractive term in van der Waals' EOS making it temperature dependent. The SRK and PR EOS added another term employing Pitzer's acentric factor, ω. Modifications of the repulsive term in van der Waals EOS are very minor for the three cubic EOS mentioned. Riazi and Mansoori, (1992) offered a modification of the repulsive term using a refractive index parameter. The goal was to better represent heavier hydrocarbons (C10+) where they claimed SRK and PR break down due to acentric factors based upon poor estimates of critical properties.

Equation (30) is a generalized form of the cubic equations discussed above. Table 4 illustrates the differences between the van der Waals, RK, SRK and PR EOS using the generalized form. When three roots are found, the largest refers to vapor, the smallest to liquid, and the third does not have a physical meaning. All roots are equal at the critical point. Various references have listed recommendations of which equation to use for which fluids (Reid, et al. 1987, Ludtke, 2004, Assael, et al. 1996, Walas, 1985).

$$Generalized\ Cubic\ EOS \quad P = \frac{RT}{V-b} - \frac{a\,\theta(T)}{(V+c)(V-d)} \tag{30}$$

Table 4: Cubic Equations of State

Name (year)	b	c	d	a	θ(T)
van der Waals (1873)	$0.125\ RT_c/P_c$	0	0	$0.421875\ R^2T_c^2/P_c$	1
Redlich/Kwong (1949)	$0.08664\ RT_c/P_c$	b	0	$0.42748\ R^2T_c^2/P_c$	$1/T^{1/2}$
Soave/Redlich/Kwong (1972)	$0.08664\ RT_c/P_c$	b	0	$0.42748\ R^2T_c^2/P_c$	$[1+(0.480+1.574\omega-0.176\omega^2)(1-T_r^{1/2})]^2$
Peng/Robinson (1976)	$0.07780\ RT_c/P_c$	$b \pm 2^{1/2} b$	$-b \pm 2^{1/2} b$	$0.45724\ R^2T_c^2/P_c$	$a[1+(0.37464+1.54226\omega - 0.26992\omega^2)(1-T_r^{1/2})]^2$

Cubic EOS can be solved analytically which makes them preferred for use in process simulators that have to iteratively solve heat and material balances for large interconnected networks of process equipment. The network solution process takes considerably longer when trial and error methods are used to determine thermodynamic properties from an EOS.

Lee Kesler Equation of State

Lee and Kesler (1975) offered an equation of state that combined several concepts discussed above. It uses the BWR EOS (or a modified BWR EOS) to calculate the compressibility factors of a simple fluid, Z^0, usually methane, and a complex reference fluid, Z^r, usually n-octane. These fluids were selected since a significant amount of measured fluid property data was available at the time for both thus giving good results by the BWR style EOS. Then the fluid of interest was introduced by use of its Pitzer acentric factor according to Equation (31) below. The concept is that the compressibility factor of a fluid can be estimated by combining the compressibility factor of a simple fluid with a ratio of acentric factors times the difference between the compressibility factors of the reference and simple fluids.

$$Lee\ Kesler\ EOS \rightarrow Z = Z^0 + \frac{\omega}{\omega^r}(Z^r - Z^0) \tag{31}$$

This EOS had some success originally, but was enhanced for mixtures when Plöcker, et al. (1978), revised the mixing rules, hence the name LKP.

Multiparameter Equations of State

Creating equations of state is highly based upon defining either theoretical or empirical relationships between mathematical models and physically measured properties of fluids. Interpolating tabulated data and/or reading values from Mollier diagrams has given way to computerized solution algorithms for determining fluid thermodynamic properties from equations of state. Also, more parameters are being used in EOS so that more measured properties can be tied to the model to improve results and usefulness. Examples are the Starling (1973) modification of the BWR EOS and the Jacobsen and Stewart (1973) *MBWR* EOS which was the first successful reference quality EOS. It provided results that were within the experimental uncertainty for nitrogen (Span, 2000).

Today, a considerable number of reference quality, multiparameter, pure fluid equations of state have been published for the fluids normally encountered in the compression industry. Span (2000) provides an excellent history of the progressive improvements that led to the *evolutionary optimization method* (EOM) for determining EOS terms from experimental values. This method coupled with using a fundamental equation of state provided many current reference quality EOS. Equations involving pressure and compressibility as functions of temperature and density have to be integrated to obtain caloric thermodynamic properties. Using Helmholtz energy, $a(T,\rho)$ as the fundamental EOS allows all thermodynamic properties to be evaluated by derivatives which makes results more easily determined. The complexity of the structure of these EOS can be seen in Equation (32) (Jacobsen, et al., 1986).

$$Multiparameter\ Helmholtz\ EOS \quad a^r(T,\rho) = \alpha^r(\tau,\delta) = \sum_{i=1}^{I_{pol}} n_i \tau^{t_i} \delta^{d_i} + \sum_{j=1}^{6} \sum_{i=1}^{I_j} n_{j,i} \tau^{t_{j,i}} \delta^{d_{j,i}} \exp(-\delta^j) \tag{32}$$

The mixing models employed rely upon high quality, binary pair interaction coefficients correlated from many experimental data samples to provide low uncertainty.

REFPROP

Thermodynamic properties for the examples included in this paper have been calculated using the REFPROP (Lemmon, et al., 2013) software from NIST, a part of the United States Department of Commerce. REFPROP implements multiple, pure substance equations of state. It is based upon multiparameter, reference quality equations of state for thermodynamic properties of individual pure fluids and a mixing rules model involving the Helmholtz energy of mixture components. It has been shown to compare very closely to high quality, measured fluid property data, an example of which can be found in McLinden (2009). Comparisons of REFPROP's thermodynamic results to several other equations of state can be found in peer reviewed technical references such as Span and Lemmon (2015) and Lemmon and Span (2010). REFPROP uses what is considered the best quality EOS for each pure fluid independent of style. These EOS and their respective qualifications are documented within the REFPROP graphical user interface.

Example Use of an Equation of State

An equation of state can not only provide fluid properties at various state points for performance calculations, but it can be used to create a fluid phase diagram showing the demarcation between gas, liquid, and two phase states. Suction and discharge operating conditions can be shown, also. An analyst needs to be able to determine how close a compressor's suction conditions are to the dew point of a fluid. Knowing discharge conditions in relation to the phase diagram can help in evaluating potential recycle line operating conditions. Figure 14 illustrates two versions of this type of display. On the left the information is displayed using customary unit scaled axes while on the right side the axis scaling has been made dimensionless by dividing the dimensional values by the critical point values. Thus, the scales on the right side are reduced pressure and temperature. The value of this display will be discussed in the method and reference section below.

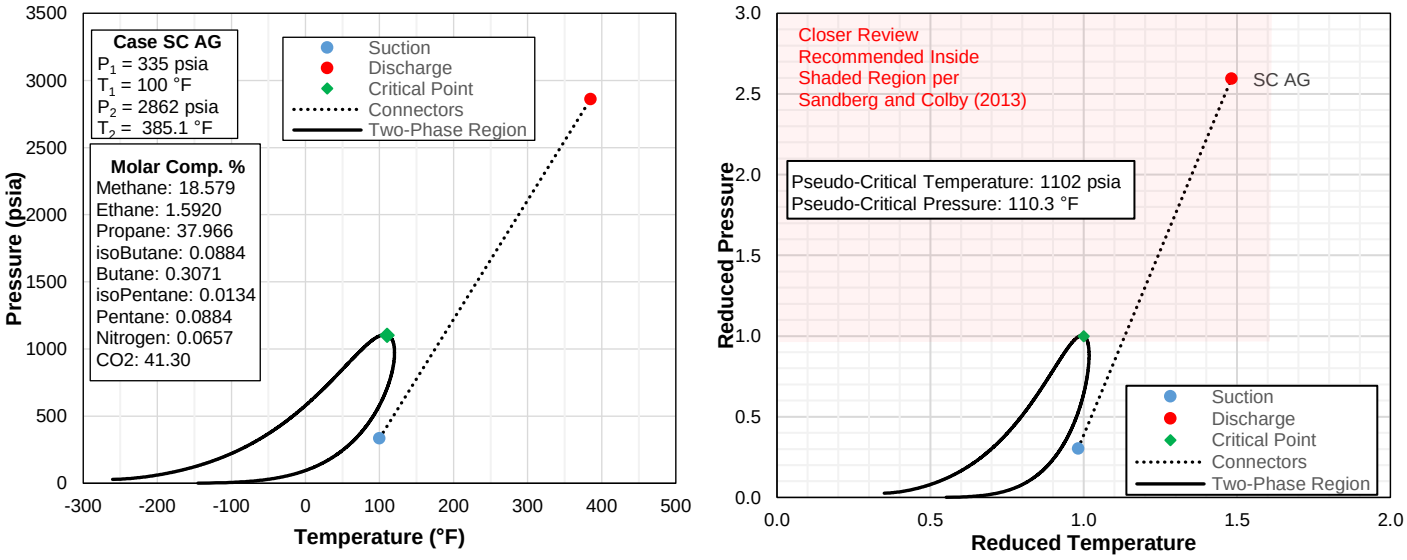

Figure 14: Pressure Temperature Graphs for Case SC AG

Both graphs in Figure 14 illustrate the critical point of the fluid and the relationship to operating conditions for a compressor. Experience has shown that equations of state can have difficulty reproducing accurate fluid properties in the vicinity of the critical point. Multiparameter equations of state designed for a particular fluid typically alleviate this problem.

A Few Final Words

Equations of state in use today for centrifugal compressor performance calculations are typically cubic such as SRK or PR, virial such as BWR, combined concepts such as LKP, or refined, multiparameter, pure fluid styles within a software package. Analytic equations (all but multiparameter mentioned above) typically have their largest deviations from measured data in the vicinity of a fluid's critical point. Unless additional terms to handle the critical point vicinity are added to an analytical EOS, any calculations in this region could be suspect.

For an analyst to make a choice of which EOS to employ, he should make an informed decision based upon an understanding of any particular EOS's capabilities and limitations. This would include knowing what accuracy to expect based upon the fluids being compressed and the operating conditions expected. A starting point for this activity is to determine the measured data limits that were used to fit an EOS's coefficients. It is good engineering practice for all parties involved to agree on an equation of state for each service. However, it must be pointed out that simply providing a name of an equation of state does not guarantee that all implementations are the same since coefficients might be developed based upon different measured data sets. Using many, reference quality, multiparameter, pure fluid EOS and a robust set of mixing rules avoids the problems that can be associated with using a one equation style fits all approach for mixtures. Above all, an analyst must not lose sight of the fact that any EOS is only a model.

Technical references that have compared compression examples using various equations of state include Hundseid, et al. (2006), Sandberg (2005), Johnson and Johansen (2009), and Kumar, et al. (1999).

REVIEW AND DISCUSSION OF SELECTED METHODS AND REFERENCES

Selected references are reviewed below in chronological order starting with Schultz's well known ASME paper (1962). Each method assumes a constant polytropic efficiency path will be followed by a compression process but evidence has shown that some path approximations are less useful. Since the overall flange to flange efficiency is the desired result, variation in efficiency along an actual compression path will not impact validity. In other words, variation along a path in the ratio of the useful energy added to a fluid to the total expended energy might vary for impellers vs. diffusers, but this is not a concern. It is the ratio of these quantities for the total process that is desired to be determined. The calculation method trend applied by these authors begins with endpoint techniques, progresses through various modifications or improvements applied to endpoint methods and moves to numerically iterative techniques of varying complexity. Some chronological overlap occurred, each attempting to illustrate better accuracy for a particular technique. Each method is described in this section and Appendix B provides additional implementation details of most of the methods mentioned below.

Schultz (1962)
Schultz realized that ASME PTC 10 (1949) employed isentropic analysis methods and did not provide for equivalent tests that could compare test stand results to expected design point field operations. He recommended rewriting the code to include polytropic analysis and equivalent testing for compressors. Test facilities could not always replicate field design conditions within a reasonable budget. Schultz's intent was to provide an analysis method that could be used to illustrate how a compressor could be shown to meet a purchasers requirements with reasonable accuracy via factory tests designed using laws of model similitude.

Schultz determined it was not possible to directly integrate Equation (1) without assuming some values were constant as implied by Equation (2). Polytropic volume and temperature exponents were held constant in addition to efficiency along a compression path since they varied much less than pressure, temperature, or volume. With over 40 differential equations included in the development he provided his polytropic analysis. Schultz realized errors were introduced due to the assumption of constant exponents and developed a correction factor. He called it the polytropic head factor which he based upon easier to calculate errors by isentropic methods resulting in closer agreement with measured test data. Two methods were shown in the paper to determine the exponents based upon the endpoints of the compression process. One of the methods described used only the compression path end points and appears to be the most common application of Schultz's methods. The second method could be used to determine exponents at individual points along the compression path and thus was used to average the exponents employed but was complicated by requiring an iterative procedure. Employing an additional midpoint along the path with the second method was an attempt to improve results by improving the path definition. Schultz included generalized compressibility charts in the paper based upon reduced pressures and temperatures to obtain compressibility functions based upon the corresponding states fluid theory to account for the lack of real gas properties for many fluids. With today's improved access to and accuracy of multiple equations of state for many fluids, application specific real gas compressibility functions are readily available based upon given fluid conditions such that the generalized charts are no longer needed. The example included in the paper made use of the third point along the compression path to improve results, but Schultz's third point method is seldom mentioned. Today, three point methods have been adapted for easier implementation.

In 1965, Schultz's methods were adopted for calculations involving compressor test data and included in ASME PTC 10 (1965) and were also retained in an updated version, ASME PTC 10 (1997). (The third point method included in Schultz's paper does not appear in the code.) Schultz's analysis provided a code that was highly useful for equivalency testing at that time.

Mallen and Saville (1977)
Mallen and Saville discussed that Schultz's method was useful at pressures below 1450 psia, but that at higher pressures it tended to violate the second law of thermodynamics for some fluids. Figure 15 demonstrates the Schultz method for compression of ethylene from 100 psia and 100 °F to 7500 psia for two values of polytropic exponent, n, using current engineering tools. It shows similar patterns to a figure developed by Mallen and Saville. As pressure increases, entropy first increases as expected but then the Schultz model predicts a decrease in entropy and reduction in temperature at high pressures. This high pressure trend does not match reality.

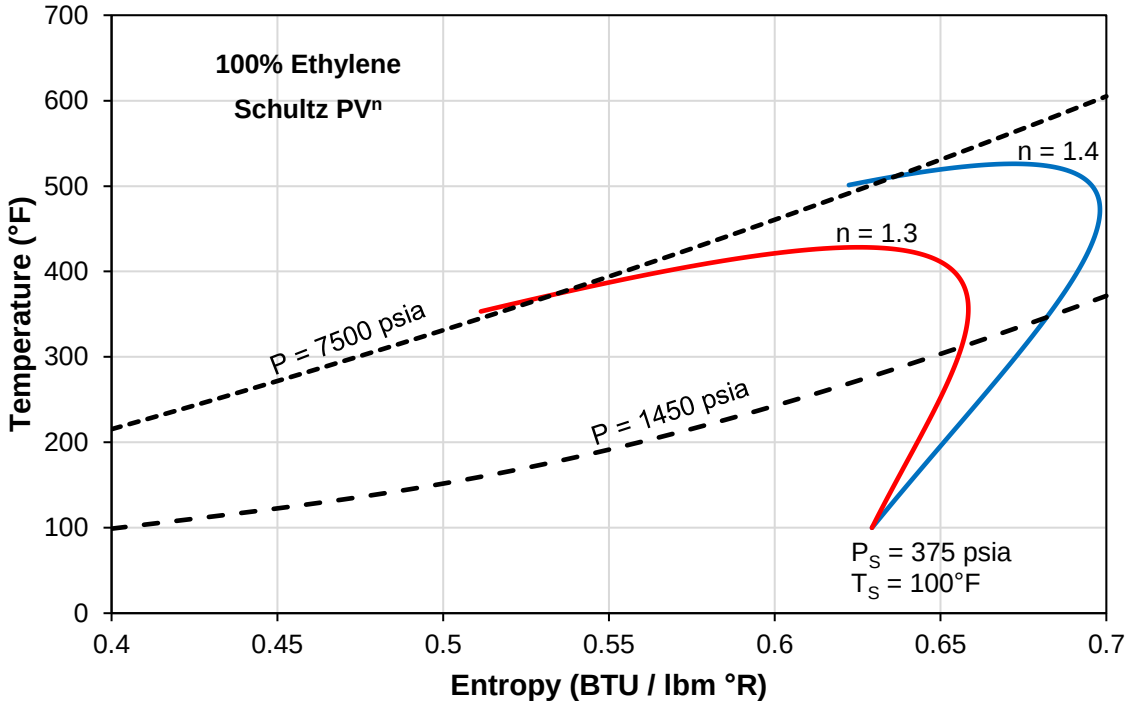

Figure 15: Schultz Method Applied to Compression of Ethylene

Mallen and Saville's end point calculation method used Equation (33) in place of Equation (2) for compression processes at high pressures. Equation (34) shows Mallen and Seville's results for use as the numerator for Equation (1). The paper compares results for Mallen and Saville's method and Schultz's method for ethylene. Their method does not require calculation of the isentropic end point values or a correction factor which makes its implementation much easier. They recommended using their method for compression above 1450 psia. Later, Huntington pointed out that their analysis required the specific heat at constant pressure be constant which defines a perfect gas. This could severely limit the ability of the Mallen and Saville method to accurately address real gases except maybe at low pressures.

$$Mallen\ and\ Saville\ Path\ Equation \rightarrow T\ \frac{dS}{dT} = Constant \tag{33}$$

$$Mallen\ and\ Saville \qquad Head_{Poly} = (H_D - H_S) - \left(\frac{(S_D - S_S)\,(T_D - T_S)}{LN\left(\frac{T_D}{T_S}\right)} \right) \tag{34}$$

Nathoo and Gottenberg (1981, 1983)

The first paper, (1981), discussed improved process variable instrumentation for operating condition measurements and provided an equation of state based approach to a so called *exact* integration of real gas equations developed by Schultz (1962). The 1983 paper rearranged two equations from Schultz and briefly describes numerical integration using a computerized RKS EOS. Equations (35) and (36) show the equations. Four example cases were presented comparing the numerical integration to Schultz's two point, constant polytropic exponent method and one was compared to Mallen and Saville's results. The conclusion was *"... in most practical cases, the assumption of n-constant leads to fairly accurate results."* Applying the numerical method in today's improved computing and equation of state environment might yield results that could impact that conclusion. The numerical solution is more cumbersome than other recently published methods discussed in this paper and is not included in the example calculations.

$$Rearranged\ Equation\ 1 \rightarrow \frac{dT}{dP} = \frac{V}{C_P}\left[\frac{1}{\eta_{poly}} + \frac{T}{V}\left(\frac{\partial V}{\partial T}\right)_P - 1\right] \tag{35}$$

$$Rearranged\ Equation\ 2 \rightarrow \frac{dV}{dP} = \left(\frac{\partial V}{\partial V}\right)_T + \frac{V}{C_P}\left(\frac{\partial V}{\partial T}\right)_P \left[\frac{1}{\eta_{poly}} + \frac{T}{V}\left(\frac{\partial V}{\partial T}\right)_P - 1\right] \tag{36}$$

Huntington (1985)
Huntington discussed why the Schultz method's polytropic head factor, f, was only correct for an efficiency of 100%. He theoretically showed that Mallen and Saville's method needed a constant specific heat at constant pressure, Cp, which eroded accuracy for real gases. Huntington offered a reference method using multiple subpaths each with a small pressure rise. He employed quadrature numerical integration of the area under a pressure volume curve along the compression path. The method was based upon a self-defining constant polytropic efficiency path rather than Equation (2). After an initial polytropic efficiency assumption, within a subpath he used an average volume to calculate vdP. He then iterated the subpath end point temperature until vdP was equal to the enthalpy change across the subpath divided by the assumed polytropic efficiency. If the final subpath endpoint temperature did not match the measured final temperature, polytropic efficiency was iterated. Once convergence was reached. Huntington summed the resulting subpath vdP values to get the numerator of Equation (1).

He pointed out in four examples that the Schultz and Mallen and Saville methods could give results that were on opposite sides of his reference results and thus might have significant errors. Huntington additionally developed a method to fit a third point to a constant polytropic efficiency path. He used a relation that assumed compressibility, Z, along the path was only a function of pressure. The iterative three point method showed close agreement with the above described reference method.

Huntington (1997)
Huntington recast the above mentioned three point method into a form that could be used to replace Schultz's polytropic head factor, f, and offered it to the ASME committee that was revising ASME PTC 10 (1965). The committee rejected the three point method based upon the fact that the revised ASME PTC 10 (1997) document was going to change the definition of polytropic compression.

This reference demonstrated an improved result for higher pressure applications. Huntington suggested that Schultz's head factor could be used in the range of $0.995 < f < 1.005$. Outside that range, he proposed using a recast version of head factor, f_h, (Equation (37)) in the range of $0.8 < f_h < 1.2$. Huntington included five example calculations and claimed accuracy improvements up to 40 times better than Schultz's head factor results. The technical paper as well as a letters exchanged between Huntington and ASME requesting the new head factor be included in ASME PTC 10 (1997) and a response declining the request are contained in the reference. Variables a, b, and c are defined in Appendix B.

$$Huntington's\ Head\ Factor \quad f_h = \frac{(H_D - H_S)/\left[\left(\frac{n}{n-1}\right)(P_D V_D - P_S V_S)\right]}{1 + \frac{(S_D - S_S)/R}{aln(P_D/P_S) + b[(P_D/P_S) - 1] + \frac{c}{2}[ln(P_D/P_S)]^2}} \tag{37}$$

Hundseid, et al. (2006)
Hundseid, et al., discussed compressor performance analysis as a lead in to wet gas compression. End point methods could not be accurately employed for wet gas compression where some portion of the fluid being compressed might change phase. The method can also be used for compression analysis of dry gas which is the subject of this current paper.

Hundseid, et al.'s paper reviews Schultz's methods and discusses that the power test code does not define how to average gas properties. (On this point, the code and Schultz's original work also appear to differ.) Illustration of multiple methods of determining average properties mixed with both Equations (4) and (5) show for isentropic analysis of a natural gas mixture, the results could differ by up to 4 %. It was pointed out that even though many sources say their work is based upon the Schultz method, the actual implementations can be different, thus providing different results for the same input data. Using five different equations of state with the end point method calculations were compared using as a basis the results from the GERG-2004 equation of state (Kunz, et al. 2007).

After considerable review and comment presented as outlined above, a small pressure step, numerical algorithm was presented that is based upon the small stage method of Equations (12) and (13). It did not average fluid properties across a pressure step as required for example in Huntington's reference method. No numeric examples were provided for the approach. A companion paper (Hundseid and Bakken, 2006) presented at the same conference gave further discussion of wet gas compression, but also did not include an example of implementation of the suggested numerical approach.

Oldrich (2010)

Oldrich used four solution methods for Equation (11) including an ideal gas model, Mallen and Saville, Schultz, and his own *"accurate"* numerical integration method using an eight coefficient BWR equation of state. The stated common theme with other references was to avoid issues encountered using a constant polytropic exponent formula. Oldrich noted a *"common incorrectness"* when using ideal gas models because of computing limits. Oldrich rearranged Equation (1) as shown in Equations (38), (39), and (40) to create a stepped numerical integration method with temperature and density inputs. He coupled Equation (38) with Equation (41) which is a simple real gas equation of state. The rearrangement helped in using the particular implementation of the BWR equation of state he had selected *"In order to enable to use arbitrary real gas equation of state…"*. (It is typical for thermodynamic equations of state to be based upon density and temperature as the internal independent variables but many equations can work with other input variables just as well by handling calculations internally to get temperature and density as inputs.) Three implementations of his numerical technique were compressor design, determining discharge conditions to evaluate if a design is within mechanical capabilities of the hardware, and compressor testing. The examples are for five pure gases: hydrogen, methane, propane, nitrogen, and ethylene. For the three mentioned end point methods, calculated efficiency and errors in the examples are compared to the compressor testing numerical iterative method and are shown graphically for a range of discharge temperatures. Using his numerical method as a basis, low errors for other methods are illustrated for hydrogen and nitrogen while large errors are found for ethylene. The Mallen and Saville method has the largest errors. Oldrich's numerical solutions techniques are more complex and thus are not included in the current example calculations.

$$\frac{d\rho}{dT} = \frac{\rho C_P - R\rho Q_T \left(\frac{1}{\eta_{poly}} + \frac{Q_T - Q_\rho}{Q_\rho}\right)}{RTQ_\rho \left(\frac{1}{\eta_{poly}} + \frac{Q_T - Q_\rho}{Q_\rho}\right)} \tag{38}$$

$$Q_T = Z + T\left(\frac{\partial Z}{\partial T}\right)_\rho \tag{39}$$

$$Q_\rho = Z + \rho\left(\frac{\partial Z}{\partial \rho}\right)_T \tag{40}$$

$$P = Z \times R \times T \times \rho \tag{41}$$

Sandberg and Colby (2013)

Sandberg and Colby demonstrated the single polytropic exponent Schultz method that the test code embraced could generate excessive errors and then defined regions of fluid reduced property conditions with higher errors. They proposed a new *polytropic correction factor* (Equation (42)) that could replace Schultz's head factor in existing calculation programs. The paper provided comparison of results for both correction factor methods and a small pressure step method based upon an iterative numerical integration solution. This numerical method was a hybrid compared to others in that it continued to use Equation (2) as a path for each small step. Included were 51 example cases that used 12 different gases. The equation of state employed was an earlier version of REFPROP (Lemmon, et al., 2013). These example cases provide sufficient input data to allow other analysts to make comparison calculations and they are included in the example cases discussed in this current paper. Sandberg and Colby clearly illustrated the error sources using three of their example cases. Then they showed why gas conditions have a different impact on each of those three cases. Their recommendation was if suction or discharge conditions were above a reduced pressure of 1.0 or below a reduced temperature of 1.6, the code's single polytropic exponent method based only upon path endpoints should not be used without modification. Sandberg and Colby's polytropic correction factor reduced errors in their example cases.

$$Sandberg\ and\ Colby\ Head\ Factor \quad f_{sc} = \frac{(H_D - H_S) - \left(\frac{T_S + T_D}{2}\right)(S_D - S_S)}{\left(\frac{n}{n-1}\right)[P_D v_D - P_S v_S]} \tag{42}$$

Taher (2014)

Taher reviewed the Schultz method and generalized compressibility charts for use if gas properties are not well known. He showed a direct calculation of compressibility functions, X and Y using the LKP equation of state. He calculated X and Y for propane and compared the results to generalized compressibility charts highlighting regions where significant differences can occur. Taher's recommendation to use specific compressibility functions illustrates a difference between Schultz's time and today in the use of graphical data. Schultz provided the generalized compressibility function charts to show a trend and to also allow an analyst to visually determine X and Y from the graphs in absence of sufficient fluid data. Today's analyst typically uses graphs to illustrate a trend but seldom to allow direct reading of a value since computing resources have rendered that activity antiquated. Taher listed the inherent irreversibility causing a temperature rise that is beyond the expected isentropic value in a compression process. This was related to reheat factors in steam turbines but was labeled a heating loss. He provided a concise definition of polytropic compression:

> *"The polytropic compression process is defined as an infinite number of infinitesimal adiabatic compression steps along the actual compression path, each step being separated from the previous step by the heating loss, while the efficiency of the overall compression process is constant and equal to each compression step."*

This definition aligns with Equations (12) and (13) and the small stage concept described in this current paper. Taher mentioned the small stage method outlined by Hundseid, et al. (2006), is the most accurate numerical calculation method since it does not include averaging gas properties within a pressure step.

Wettstein (2014)

Wettstein compared three polytropic calculations methods for air and five pure gases: neon, argon, oxygen, nitrogen, and carbon dioxide. He compared results for the ideal gas, constant polytropic exponent (Schultz), and stepwise numerical integration method solutions for Equation (1). His numerical solution, labeled a *Constant Dissipation Rate Algorithm* (CDRA), is a formal description of polytropic efficiency being constant throughout the compression process. This fits the current paper's concept since it is applied on a flange to flange basis. (The constant polytropic efficiency concept cannot represent analysis of a series of internal compressor components such as impellers and diffusers since their individual efficiencies are typically different.) Wettstein provided developmental history of CDRA going back to Zeuner (1905) and Stodola (1910).

Wettstein averaged temperatures for a step and then used step pressure to calculate a step volume change with an equation of state. Temperature was iterated for each step. Based upon given inlet and outlet temperatures and pressures, polytropic efficiency was iterated until the correct final calculated temperature was achieved. Varying the number of steps to reach a sufficiently converged solution yielded a value of 100 steps could be applied to determine a final temperature within acceptable tolerances. One interesting conclusion was that a gas with more atoms in its molecule would converge faster for his examples. Examples included compression from 1 bar to 100 bar for several efficiencies. The largest errors were found for air and carbon dioxide. Ideal gas solutions had fairly large errors while the Schultz method had up to 1.5 percent errors under some conditions. Wettstein recommended a numerical integration method be used and for all parties of a particular project be consistent. Wettstein's numerical solution is a variation of Huntington's reference method discussed in this paper and was not included in the example calculations discussed below.

Plano (2014)

Plano's subject for his Master's Degree Thesis was models for wet gas compression. He used the Hundseid, et al. (2006), small stage algorithm. An example comparing the impact of several equations of state on results for dry and wet gas analyses was included. This reference and one other (Xi, et al., 2009) are the only easily obtainable references prior to 2017 that were found containing numerical examples that implement Hundseid, et al.'s (2006), algorithm for a small stage method.

Final Comment

Literature searches for publications showing implementation of the Hundseid, et al. (2006), small stage algorithm yielded only two numeric example cases but multiple textual comments as to its high accuracy. In the course of developing this paper, this particular small stage method implementation has proven to be highly accurate and simple to solve in a spreadsheet format. Results based upon a 100 incremental step version of this method are the basis for comparison of other methods applied to examples presented in this paper.

ILLUSTRATIVE EXAMPLES

Each of the first eight centrifugal compressor performance analysis methods listed in Table 3 above have been employed to analyze 70 example cases covering 16 different gases. The compositions cover both pure fluids and mixtures typically encountered in the turbomachinery industry.

Five end point methods and three iterative, numerical, pressure step methods are included. Two of the numerical methods include multiple calculations using different numbers of steps. This yields 12 calculations for each example case that have been implemented in a spreadsheet format. The calculations that require iterative solutions have been addressed by algorithms embedded in the spreadsheet macro language. A common, non-limiting assumption is constant polytropic efficiency and each method must determine a compression path, polytropic head and efficiency using the same software implementation of reference quality equations of state.

Some of these example cases came from several references reviewed above and others were created for this paper. For known inputs of fluid composition and suction and discharge pressures and temperatures, polytropic head and efficiency were calculated. Pressures and temperatures are for stagnation conditions. See Appendix A of ASME PTC 10 (1997) for a discussion of using stagnation conditions to define compressor performance. To make relative comparisons, results from the 100 step Small Stage method were used as reference values. Table 6 and Table 7 in Appendix C document the fluid compositions, pressures and temperatures, and resulting percentage deviations for each calculation.

Figure 16 provides a comparison of reduced pressures and temperatures for suction and discharge for each example case. Also noted is the region identified by Sandberg and Colby that requires closer attention ($P_r > 1.0$ and $T_r < 1.6$). Note that the refrigerant 12 example from Schultz (1962) can be seen in the bottom left corner of the figure, well away from areas of concern for using end point methods.

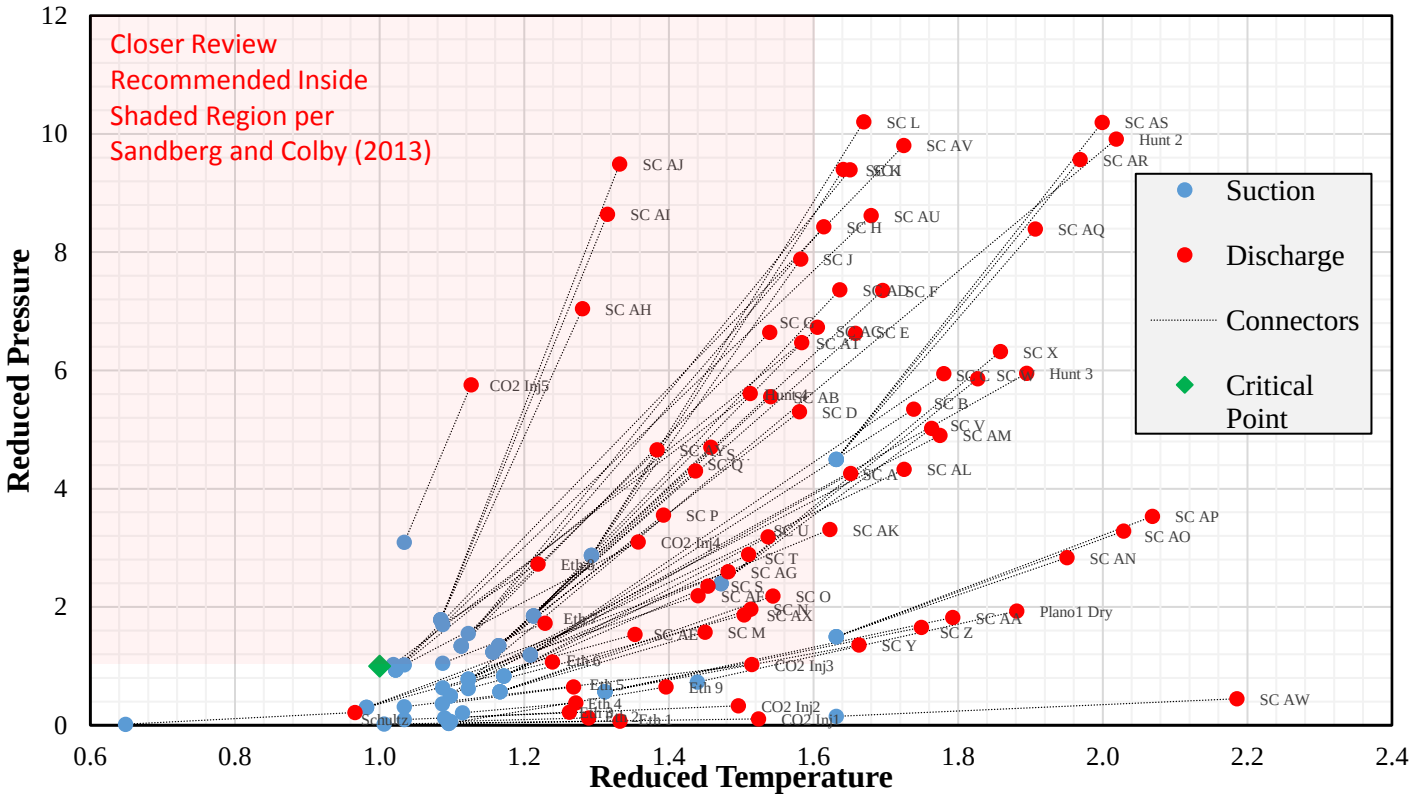

Figure 16: Reduced Pressures and Temperatures for Suction and Discharge Conditions for 70 Example Cases

An example of the 12 individual calculations is shown in Figure 17 which is for Case SC AG, a high compression ratio case. The fluid is a mixture dominated by CO2, propane and methane. The largest error is 6.8% produced by Schultz's XY end point method that averages the polytropic exponents determined at suction and discharge conditions. The phase diagram of Figure 14 shows that the operating conditions and compression path for this case reach well into the region identified by Sandberg and Colby where closer attention is required. Both the Schultz and Sandberg Colby single exponent methods have head factors of approximately 0.96 which is another indication of potential error since they are not near 1.0. Huntington's three point method shows respectable results. Results for all numerical pressure step methods are seen to be small compared to end point methods. This was true for all example cases.

Also, listed in Figure 17 are elapsed time results for the iterative methods. Typically, more pressure steps require longer solution times and iterative methods with nested loops take more time than the small stage method. The actual values shown are dependent upon the programmed numerical solution algorithms. A combination of the spreadsheet software's built in solutions and an analyst programmed Newton Raphson secant method was used for methods requiring nested iterations. Other algorithms would likely have different results. The fluid mixture for Case SC AG is a somewhat difficult mixture for equations of state and they have their own embedded numerical methods that must reach convergence. Thus the elapsed times reflect this. Calculations for a pure fluid would likely be much faster since mixing rules would not be involved and the saturation curve coordinates are usually well known.

Calculated Polytropic Performance

Method	Converge?	English Units Head ft lbf / lbm	English Units Efficiency %	Metric Units Head kJ / kg	Metric Units Efficiency %	Polytropic Head Error %	Polytropic Head Error ft lbf / lbm	Elapsed Time seconds
Schultz Endpoints		48454.3	81.550	144.73	81.550	-0.598	-292	NA
f_s (Polytropic Head Factor)		0.96005		0.9594				
Schultz Endpoints (X,Y)	0	52056.7	87.613	155.53	87.632	6.792	3311	0.156
Sandberg Colby Endpoints		48696.7	81.958	145.46	81.958	-0.101	-49	NA
f_p (Polytropic Correction Factor)		0.96485		0.9642				
Sandberg Colby 20 Step Integration	0	48736.6	82.025	145.58	82.025	-0.019	-9	51.121
Mallen Saville Endpoints		48845.7	82.209	145.90	82.209	0.204	100	NA
Huntington 3rd point	0	48715.1	81.989	145.51	81.989	-0.063	-31	1.279
Huntington 20 Step Integration	0	48713.7	81.987	145.51	81.987	-0.066	-32	91.463
Huntington 50 Step Integration	0	48729.1	82.013	145.56	82.013	-0.035	-17	236.019
Huntington 350 Step Integration	0	48732.0	82.018	145.56	82.018	-0.029	-14	1628.691
Small Stage 20 Steps	-0	48667.2	81.909	145.37	81.909	-0.162	-79	12.995
Small Stage 50 Steps	0	48726.6	82.009	145.55	82.009	-0.040	-19	33.166
Small Stage 100 Steps	-0	48746.0	82.042	145.61	82.042	0	0	69.825

Figure 17: Example Case SC AG Results for Centrifugal Compressor Performance by 12 Calculation Methods

Table 5 provides an overview of results for all 70 example cases and two composition subgroups, high CO2 content (>40%) and ethylene. Minimum, maximum, and average errors for each method are listed. The reference method is the 100 step Small Stage method. The superiority of the numerical methods over the end point methods is evident. The Huntington 3 point method fairs better than the other end point methods.

Table 5: Errors for Three Groups of Examples

	All 70 Case Errors			High CO_2 Case Errors			Pure Ethylene Case Errors		
	Min %	**Max %**	**Avg %**	**Min %**	**Max %**	**Avg %**	**Min %**	**Max %**	**Avg %**
Schultz	-1.80	0.25	-0.31	-1.35	0.06	-0.47	-1.80	-0.00	-0.36
Schultz XY	-0.71	15.6	1.05	-0.08	6.79	1.64	-0.09	15.56	2.14
Sandberg Colby	-0.39	0.46	0.09	-0.39	0.46	0.13	-0.15	0.18	0.01
Sandberg Colby 20 Step	-0.06	0.04	-0.03	-0.05	0.04	-0.02	-0.06	0.02	-0.04
Mallen Saville	0.03	1.17	0.29	0.06	1.17	0.43	0.03	0.89	0.24
Huntington 3 Point	-0.21	0.12	-0.02	-0.21	0.12	-0.03	-0.20	0.08	-0.02
Huntington 20 Step	-0.13	0.04	-0.04	-0.07	0.04	-0.03	-0.13	-0.03	-0.06
Huntington 50 Step	-0.06	0.03	-0.04	-0.05	0.03	-0.03	-0.06	0.00	-0.04
Huntington 350 Step	-0.06	0.02	-0.04	-0.05	0.02	-0.03	-0.06	0.01	-0.04
Small Stage 20 Step	-0.37	-0.05	-0.13	-0.37	-0.08	-0.17	-0.30	-0.05	-0.12
Small Stage 50 Step	-0.09	-0.01	-0.03	-0.09	-0.02	-0.04	-0.08	-0.01	-0.03

Note: Reference values provided by the 100 Step Small Stage Method.

The largest error in Table 5 is 15.6% for ethylene using the Schultz XY end point method. This case is actually from Huntington (1985) and Mallen and Saville (1977) and has a pressure ratio of 20. It is similar to the case shown in Figure 15. The case is useful for evaluating calculation methods as it accentuates the problems with end point methods. However, it is unlikely that a centrifugal compressor would be built to do this work in one uncooled stage. Ethylene has historically been considered a difficult fluid for which to predict thermodynamic properties. Brown (1997) has labeled it *unruly* since "*the k value from point 1 to point 2 is highly nonlinear*." This obviously refers to Schultz style analyses, but the concept is correct.

Ethylene

Thermodynamic properties of fluids typically show their highest variation near the critical point and ethylene is no exception. Figure 18 shows the variation of specific heat, C_p, for ethylene in the vicinity of the critical point which illustrates it is a function of both pressure and temperature. The critical temperature of ethylene is 48.56 °F which is in a range of potential compressor suction temperatures. In this region, even small temperature changes yield very large changes in thermodynamic properties like C_P and density. Rapidly changing C_p and density due to minor suction temperature variations could be the phenomenon at the root of Brown's *unruly* label for ethylene. The temperature range used to create Figure 18 was 1.4 °F and the range for C_p is seen to be from 0.4 to over 45 BTU / lbm °R, a factor of 112. The values shown depend upon the temperature steps chosen and may not reveal the maximum. See Sengers and Sengers (1968) for further discussion of this phenomena which can show a discontinuity at the critical point. These issues coupled with a calculation method that is based only upon compression end point conditions on either side of the critical point could likely be the *perfect storm* for performance analysis of a centrifugal compressor, especially if a mediocre EOS is used.

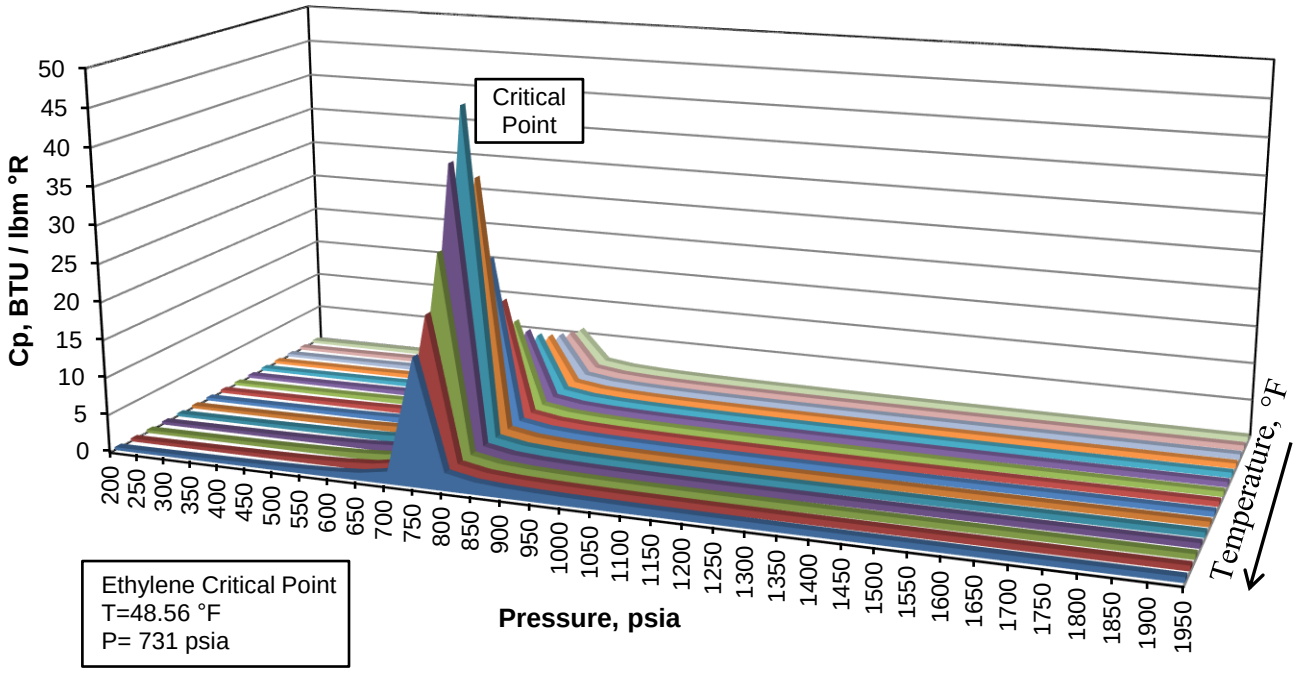

Figure 18: Variation of Specific Heat for Ethylene

Carbon Dioxide

Carbon dioxide is another fluid that has been considered a problem for the same reasons discussed above for ethylene since its critical temperature is 87.76 °F. Adding small amounts of diluents such as hydrocarbons can slightly lower the critical temperature. The peak value for C_p for CO2 near its critical point is over 18000 BTU / lbm °R and a graph would look similar to Figure 18. The impact of small suction temperature fluctuations upon density of CO2 in the vicinity of its critical point is shown in **Figure 19**. Shown are suction data points for four stages of compression for carbon dioxide from near atmospheric conditions. Isobars between 1000 and 2000 psia are also shown. The fourth stage suction conditions are 95 °F and 1100 psia which is near the critical point for CO2. The fourth stage suction stream comes from an air cooled exchanger which could allow some variation in suction temperature due to changing weather conditions. As suction temperature decreases, suction density increases rapidly along a constant pressure line of 1100 psia. If the temperature drops by 5 °F to point 4`, the density increases by 37%. This translates into a compressor suction volume flow decrease of an equal percentage magnitude which could drive the fourth stage operating point to surge.

Head calculation errors in this vicinity of a fluid's critical point can be significantly reduced by using numerical pressure step methods (Evans and Huble, 2017). However, just being able to perform acceptable head calculations does not mean these designs are robust and could operate without difficulty.

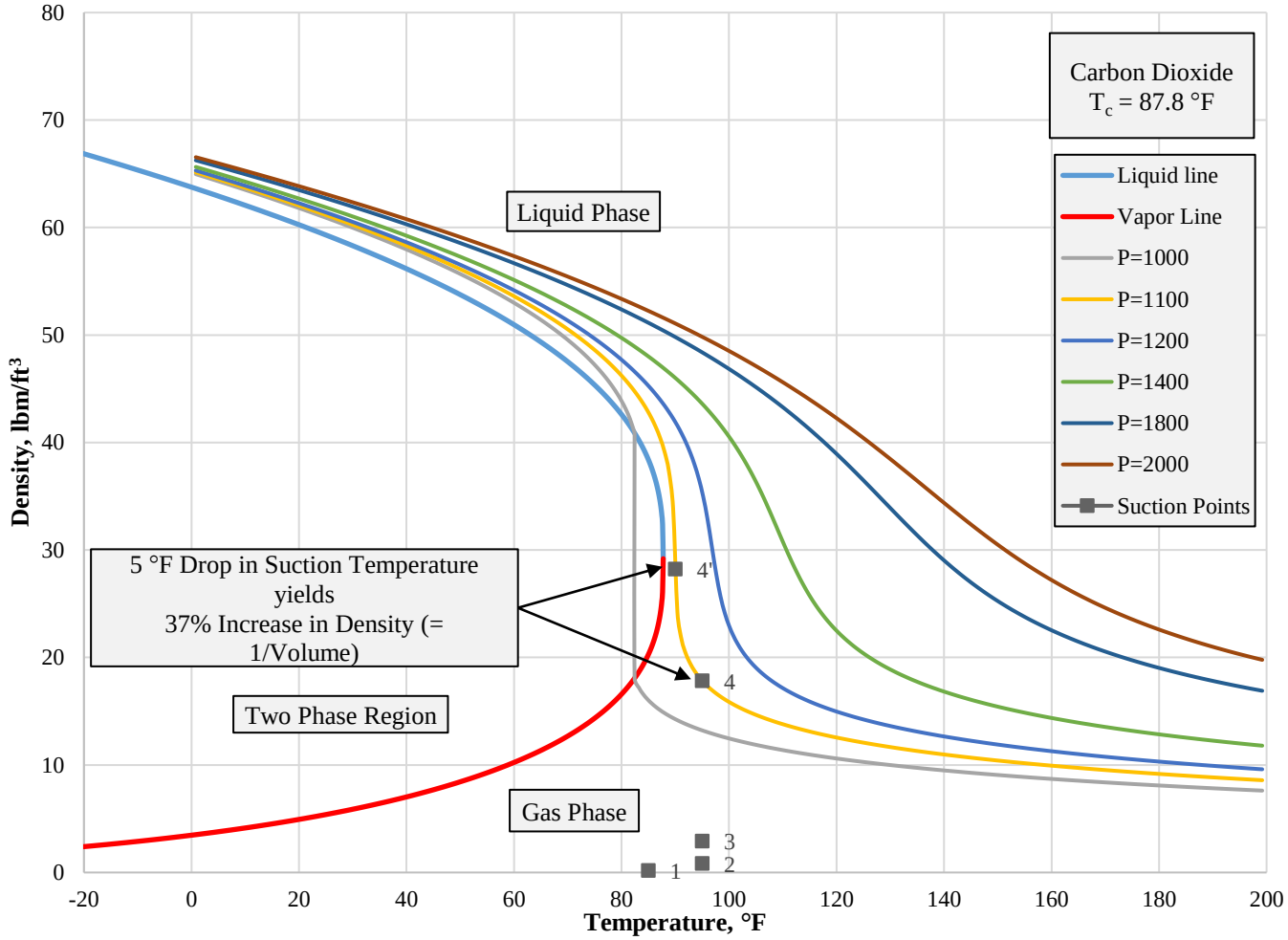

Figure 19: Variation of Density as a Function of Temperature and Pressure for Carbon Dioxide

CONCLUSIONS

Models for centrifugal compressor performance analyses can employ either end point style or numerically iterative methods to determine polytropic head. Numerical methods have been shown to provide superior results for flange to flange calculations that determine an overall constant efficiency along the compression path. The accuracy of the results are impacted by the quality of the thermodynamic equation of state employed.

The current ASME Power Test Code 10 (1997) embraces end point methods developed by Schultz (1962) when engineering tools for calculations and fluid thermodynamic property data were limited. These methods are based upon assumptions needed at the time to obtain solutions. Today these limitations and the need for some assumptions have been removed by computing advancements and reference quality equations of state that are accessible to analysts at relatively low cost.

Analysts should arm themselves with sufficient knowledge and background concerning methods and models used for performance analyses to allow informed decisions to be made concerning acceptance of aerodynamic compressor tests as well as acceptance of the compressor itself to perform the intended duties.

NOMENCLATURE

Acronyms

ASME	American Society of Mechanical Engineers
BWR	Benedict, Webb, Rubin equation of state
BWRS	Benedict, Webb, Rubin, Starling equation of state
CDRA	Constant Dissipation Rate Algorithm
DIA	Direct Integration Approach
EOM	Evolutionary Optimization Method
EOS	Equation of State
ISO	International Organization for Standardization
MBWR	Jacobsen and Stewart equation of state
NIST	National Institute of Standards and Technology
PR	Peng-Robinson equation of state
PTC 10	ASME Power Test Code 10
REFPROP	Reference Properties (NIST implementation of multiple reference quality EOS)
RK	Redlich-Kwong equation of state
RKS	Redlich-Kwong-Soave equation of state
SC	Sandberg Colby

Variables

a	Coefficient in Huntington's three point method, also used as a constant in van der Waals' equations
b	Coefficient in Huntington's three point method, also used as a constant in van der Waals' equations
c	Coefficient in Huntington's three point method
C	Specific Heat
d	Mathematical differential operator
E	Energy of a system
f	polytropic head factor
g	Gravitational acceleration
i	Subpath step
j	Number of subpath steps in compression path
k	Ideal gas isentropic exponent = C_P / C_V
H	Enthalpy
h	Specific enthalpy
KE	Kinetic Energy
m	Temperature exponent
MW	Molecular Weight
n	Volume exponent
P	Pressure
PE	Potential Energy
PR	Pressure Ratio
PvTx	Pressure, volume, Temperature, composition
Q	Heat input to a system
R	Gas Constant = R_0 / MW
S	Entropy
s	Specific Entropy
T	Temperature
U	Internal Energy
u	Specific Internal Energy
V	Volume
v	Specific Volume
W	Work done by a system

X	Coefficient of volume expansivity function
Y	Coefficient of isothermal compressibility function
z	Elevation
Z	Compressibility factor
Δ	Change (Difference between two points)
δ	Mathematical small difference operator
∂	Mathematical partial differential operator
η	Efficiency
ρ	Density
ν	Velocity
ω	Pitzer's acentric factor

Subscripts

Avg	Average
c	Critical
D	Discharge Conditions
h	Huntington
i	Step value (also i+1 next step, and i-1 previous step)
j	Number of steps
isen	Isentropic
Mid	Midpoint in a three point method
new	Next value in recursive formula
P	Constant Pressure
poly	Polytropic
r	Reduced
S	Suction conditions
sat	Saturated vapor
T	Constant Temperature
V	Constant Volume
0	Universal

Superscripts

0	Simple fluid
r	Complex reference fluid

APPENDIX A – NOTES AND COMMENTS ON SELECTED COMPRESSOR PERFORMANCE PAPERS

Centrifugal compressor performance calculation methods have been the subject of or partially discussed in over 35 publications in previous Turbomachinery Symposia proceedings. The following brief comments are based upon reviews of selected works. This list is not exhaustive but is representative of the coverage the subject has received by Turbomachinery Symposia publication authors. These publications partially reflect the historical progression of industry publications on centrifugal compressor performance related to the oil and gas segment. Over the 45 years the Symposia have been held, there are several 4 and 5 year gaps when the subject of centrifugal compressor performance appears to have been absent from the published proceedings. Granted the subject is not on the cutting edge of groundbreaking technology, but current work seems to be concentrated on iterative numerical methods as driven by the desire for improved accuracy and handling two phase fluids for wet gas compression.

Publications from other technical venues are not included here as this list is intended as an overview of the subject in the Turbomachinery Symposia only. Several key historical publications that directly deal with the calculation methods illustrated in this paper are reviewed elsewhere in this paper.

Not all of these publications deal with determination of centrifugal compressor head and efficiency which is the main subject of this paper. Many of the ones that do touch on the subject typically use equations that were easy to implement at the time of publication. These are not always the best current approach since the tools now available to an analyst have improved greatly over the years. That is not to say the information presented is incorrect, but the reader is cautioned to be cognizant of any limitations imposed by the selected methods in any individual publication.

The first publication concerning compressor performance at a Turbomachinery Symposium was presented by Boyce (1972) and dealt with losses in various rotating and stationary parts within the gas flow path. It did not delve into the flange to flange efficiency calculations that are the subject of this presentation.

Thompson (1972) discussed turbine aerodynamics and efficiencies, labeling the latter *figures of merit*. He outlined the *small stage* concept for an expansion process in a turbine utilizing an enthalpy vs. entropy (HS) diagram but the presented equations reveal it was in light of an ideal gas. A reheat factor was identified to relate isentropic and polytropic efficiencies for a turbine stage. Some discussion was included regarding divergence of isobars in a HS diagram. The small stage concept can be applied to a real gas compression process in a numerical summation as described in other sections of this current paper.

Davis (1973) discussed field data acquisition and evaluation. He introduced concepts from ASME PTC 10 (1965) and mentioned two issues. First, the ratio of specific heats for a real gas is not constant throughout a polytropic compression process. The second issue was that determining enthalpy rise between the end points of a compression process was difficult, especially for mixtures due to the small amount of published fluid data. Today, both of these issues have been resolved, but an analyst must beware of the calculation methods employed. Otherwise, the same problems faced over 40 years ago could manifest in current results.

Pais and Jacobik (1974) and Boyce, et al. (1976), presented field testing and data processing techniques as related to ASME PTC 10 (1965) including generalized compressibility charts.

Stanley and Bohannan (1977) illustrated use of dynamic simulation of compressor and piping systems to model control of large power machines. This applied compressor performance calculations to non-steady state operating conditions and assisted in design and sizing of facility flow path elements external to a compressor. One interesting stated conclusion was that hybrid (combined analog and digital) computers were better suited to the task than fully digital computers due to a perceived superior interaction between analyst and computer. One would be hard pressed today to find an analog computer in use for compressor analysis.

Nathoo and Gottenberg (1981) presented a case for more accurate performance calculations for hydrocarbon mixtures using improved instrumentation for gas composition determination, a computer coded equation of state (EOS), and a numerical integration method. (A later, non-Turbomachinery Symposium publication (Nathoo and Gottenberg, 1983) described details of the numerical method.) The resulting computer code accessed both the EOS and the numerical method using an interactive interface for measured data input and results output. The conclusion was that the methods embraced by ASME PTC 10 (1965) were sufficient.

1981 was a watershed year for compressor performance field testing publications at the tenth Turbomachinery Symposium. One Lecture (see previous paragraph) and seven Tutorials were presented. Clark (1981) actually titled a subsection of his tutorial "No Accurate Way to Calculate for Real Gas Mixtures." His conclusion was that field monitoring of performance did not need to be of the same quality as highly controlled shop testing, but rather that a consistent field applied method was sufficient for trending. Hunt (1981), discussed the fact that field measured performance falls off with time and should be quantified by periodic accurate testing in his tutorial.

Shop full load testing and recommended additional restrictions for an ASME PTC 10 Type 1 test are discussed by Maretti, et al. (1982). Shop test compression paths for various gases applying only the code requirements are compared to the design compression path. Adding additional restrictions for limits on test gas parameters showed better adherence to the intent of the test code.

Duggan (1987) provided a case history of the usefulness of online and offline performance monitoring. This appears to be the only publication dealing with compressor performance at the Turbomachinery Symposia over a 9 year period from 1983 to 1991.

Ludtke (1992) documented a modular design system for centrifugal compressors and claimed 97 percent of the installations designed with his system over a 20 year period were operated successfully without modifications. The system is based upon a standard line of scalable, fixed geometry components that operate under limited deviations from the principles of aerodynamic similarity.

Many ASME PTC 10 Class II compressor performance tests before the mid-1990s were performed with Refrigerant 22. A shift to more environmentally friendly inert test gases was the subject of a paper by Aicher (1993) in which he illustrated good agreement of test results using Refrigerant 134a. This refrigerant is still in use today for many tests.

Boyce (1993) briefly discussed compressor efficiencies from a perfect gas standpoint and identified polytropic efficiency as the small stage or infinitesimal stage efficiency. The paper highlighted factors that affect efficiency.

A case history of an aerodynamic design problem existing and being discovered during testing despite following previously established design criteria is the subject of a paper by Sorokes, et al. (1994). Stall related problems were traced back to stationary hardware components. The value of Class I testing was demonstrated.

Brown and Lewis (1994) provided an estimation method for sizing and modeling centrifugal compressors. The conclusion was that it only provided a rough estimate and that having a manufacturer do a formal sizing exercise would be required after the screening criteria was applied to various vendor's catalog data.

Prior agreement between the compressor manufacturer and the end user regarding field testing procedures and acceptance criteria was emphasized in a lecture by Kurz and Brun (1997). A similar subject was presented as a tutorial two years later (Kurz, et al., 1999). Kurz and Brun (2005), is a similar lecture.

Shah and Bartos (1997) discussed confirmation of impeller performance using test data and computational fluid dynamics (CFD). After qualifying the CFD model, further investigations into losses can be helpful in improving the design.

Ludtke (1997) provided a review of methods to rerate a compressor that is already in operation.

Although it is not listed in the online database of Symposia proceedings, a short course was conducted by Keenan, et al. (1998), dealing with the then new version of ASME PTC 10 (1997). The topics covered included a broad range of subjects concerning shop testing of centrifugal compressors and calculation of results. Example calculations were shown employing computerized spreadsheets which included not only the parameter values but also the equations applied in spreadsheet row/column format.

Wilcox (1999) discussed practical methods of performance field testing with flow charts for procedures and a section on troubleshooting guidelines. He pointed out the need to trend many points over time to assist in maintenance activity scheduling. The test codes and methods to estimate compressor head discussed in this paper and most other references deal with compression of dry gas which usually has a scrubber vessel upstream of the suction nozzle. As the offshore industry aims to employee subsea compression, the separation of liquids from the gas stream is not assured.

Brenne et al. (2005), compared a method for calculation of compressor performance of dry gas with a proposed method that accounted for a small percentage of liquid in the flow stream. Testing results with up to 5 % liquid volume fraction were reported.

Equation of State influence on performance results was the subject presented by Sandberg (2005) in which he showed how calculation of test results varied when four different equations of state were employed. Not all situations can be handled with the required accuracy by one equation of state and care must be taken when selecting the analysis approach.

Colby (2005) discussed shop performance testing assumptions and inherent errors based upon his extensive experience.

Starting around 2007, several short courses on aerodynamic performance and centrifugal compressor basics have been offered many times but the publications are not available in the open technical literature.
Rasmussen and Kurz (2009) provide a quick overview of compressor calculations for isentropic and polytropic paths. The paper then discusses various applications in upstream and mid-stream sectors with examples given in several appendices.

A comprehensive review of the inherent limitations of ASME PTC 10 (1997) and reasons behind them was presented by Sandberg and Colby (2013). Many test cases were shown and the data made available for further use by future analysts. Under some conditions, the ability of the Schultz methods embraced by ASME PTC 10 were shown to incur significant errors. A new correction factor was proposed to replace the Schultz head factor. Additionally, to provide an accurate evaluation of the methods, an iterative numerical integration method was shown. This current paper makes use of the test cases presented.

Sorokes (2013) discussed the tradeoffs of compressor operating flow range versus peak efficiency. The equations used are referenced for a thermally perfect gas. Determining polytropic efficiency of a real gas is described as "*a far more complicated effort*." This tutorial presentation was repeated in 2015.

Sorokes, et al. (2014) described mechanical and aerodynamic issues to consider when revamping an existing compressor. Similar to the above presentation from 2013, the equations refer to a thermally perfect gas and mention the difficulties of dealing with a real gas.

APPENDIX B – IMPLEMENTATION OF POLYTROPIC HEAD CALCULATION METHODS

Three initial steps are common to the methods listed below (except for Oldrich's first and second methods) and are stated here to avoid duplication. Pressures and Temperatures discussed below are assumed to be for stagnation conditions. See Appendix A of ASME PTC 10 (1997) for a discussion of using stagnation conditions to define compressor performance.

A. Given suction and discharge temperatures and pressures and gas composition, T_S, P_S, T_D, P_D, mol%, MW
B. Select an equation of state that can calculate the required thermodynamic variables based upon available inputs.
C. Calculate variables for the suction and discharge conditions, V_S, H_S, S_S, Z_S, V_D, H_D, S_D, Z_D and reduced properties T_{Sr}, P_{Sr}, T_{Dr}, P_{Dr} using the EOS selected in the previous step.

Schultz Method 1

1. Calculate isentropic discharge temperature, T_{Disen}, Volume, V_{Disen}, and enthalpy, H_{Disen}, using P_D and S_S in calls to the EOS.
2. Calculate polytropic exponent, n, using Equation (5).
3. Calculate real gas isentropic exponent, n_{isen}, using Equation (43) below.
4. Calculate polytropic head factor, f, using Equation (10) below.
5. Calculate uncorrected polytropic head, $Head_{poly}$, using Equation (4).
6. Multiple $Head_{poly}$ from step 5 by f from step 4 to get a value for the numerator in Equation (1).
7. Use Equation (1) to calculate polytropic efficiency, η_{poly}, by dividing result of step 6 by ($H_D - H_S$).

$$Real\ Gas\ Isentropic\ Exponent = n_{isen} = \frac{LN\left(\frac{P_D}{P_S}\right)}{LN\left(\frac{V_S}{V_{Disen}}\right)} \tag{43}$$

$$Polytropic\ Head\ Factor = f = \frac{H_{Disen} - H_S}{\left(\frac{n_{isen}}{n_{isen}-1}\right)\left(P_D V_{Disen} - P_S V_S\right)} \tag{10}$$

Schultz XY Method

1. Calculate isentropic discharge temperature, T_{Disen}, Volume, V_{Disen}, and enthalpy, H_{Disen}, using P_D and S_S in calls to the EOS.
2. Assume an initial polytropic efficiency as a constant value along the path.
3. Calculate compressibility functions X and Y for suction and discharge conditions using Equations (6) and (7).
4. Calculate polytropic temperature and volume exponents, m and n, for suction and discharge conditions using equations (8) and (9) and X, Y, from step 3.
5. Calculate $n_{avg} = (n_S + n_D) / 2$ from step 4 results.
6. Calculate compressibility functions X and Y for isentropic discharge conditions using Equations (6) and (7).
7. Calculate isentropic temperature and volume exponents, $m_{D\ isen}$ and $n_{D\ isen}$, for isentropic discharge conditions using equations (8) and (9) and X, Y, from step 6 with $\eta_{Poly} = 1$.
8. Calculate $n_{isen\ avg} = (n_S + n_{D\ isen})$ from the results of step 7.
9. Calculate polytropic head factor, f, from equation (10) using results from step 8.
10. Calculate uncorrected polytropic head, $Head_{poly}$, using Equation (4) and n_{avg} from step 5.
11. Multiple $Head_{poly}$ from step 10 by f from step 9 to get a value for the numerator in Equation (1).
12. Use Equation (1) to calculate polytropic efficiency, η_{poly}, by dividing result of step 11 by ($H_D - H_S$).
13. Iterate efficiency until assumed value in step 2 equals calculated value from step 12.

$$Compressibility\ Function\ X = \frac{T}{V}\left(\frac{\partial V}{\partial T}\right)_P - 1 \;=\; T \times (volume\ expansivity) - 1 \tag{6}$$

$$Compressibility\ Function\ \ Y = -\frac{P}{V}\left(\frac{\partial V}{\partial P}\right)_T = P \times (isothermal\ compressibility) \tag{7}$$

$$Polytropic\ Temperature\ Exponent\ \ m = \frac{Z \times R}{C_P}\left(\frac{1}{\eta_{Poly}} + X\right) \tag{8}$$

$$Polytropic\ Volume\ Exponent\ \ n = \frac{1}{Y - m(1+X)} \tag{9}$$

Mallen and Saville Method

1. The numerator of Equation (1) is calculated by Equation (44).
2. Dividing the results of step 1 by ($H_D - H_S$) gives efficiency.

$$Head_{Poly} = (H_D - H_S) - \left(\frac{(S_D - S_S) \times (T_D - T_S)}{LN\left(\frac{T_D}{T_S}\right)}\right) \tag{44}$$

Huntington Reference Stepped Numerical Integration Method

1. Assume an initial polytropic efficiency as a constant value along the path.
2. Select a number of equal pressure ratio steps i between suction and discharge and calculate the pressure ratio using Equation (14).
3. Increment pressure P_i and estimate a temperature, T_i, at the next step.
4. Calculate V_i, H_i, S_i based upon P_i and estimated T_i.
5. Calculate an average volume using Equation (45).
6. Calculate Equations (46) and (47)
7. Iterate temperature T_i for the step until the change in enthalpy (H_i-H_{i-1}) times the estimated efficiency (Equation (47)) equals the volume (V_{avg}) times the change in pressure (Pi-P_{i-1}) (Equation (46)) within a small tolerance.
8. Repeat steps 3, 4, 5, 6, and 7 for all pressure increments.
9. Compare the final discharge temperature to the given value, T_D.
10. Increment efficiency and repeat steps 3, 4, 5, 6, 7, 8, and 9, until the final discharge temperature error is within a given small tolerance.
11. Calculate $Head_{Poly}$ from Equation (48).
12. Use Equation (1) to calculate polytropic efficiency, η_{poly}, by dividing result of step 11 by ($H_D - H_S$).

$$V_{Avg_i} = \frac{V_i + V_{i-1}}{2} \tag{45}$$

$$Head_{Poly_i} = V_{Avg_i}(P_i - P_{i-1}) \tag{46}$$

$$Head_{Poly_i} = \eta_{Poly}(H_i - H_{i-1}) \tag{47}$$

$$Head_{Poly} = \sum_{i=1}^{j} Head_{Poly_i} \tag{48}$$

Huntington Three Point Method

1. Calculate Equations (49) and (50) to get an approximate midpoint in the compression path.
2. Calculate an initial value for S_{Mid} with an equation of state using the results of step 1.

3. Calculate Z_{Mid} with an equation of state using the results of step 1.
4. Calculate b, a, and c from Equations (52), (51), and (53).
5. Calculate an estimate of polytropic efficiency and head using Equations (54) and (55).
6. Calculate d, e, and $S_{Mid\ new}$ using Equations (56), (57), and (58).
7. Calculate a new estimate of the midpoint temperature using Equation (59).
8. Repeat steps 3, 4, 5, and 6.
9. If the values of polytropic efficiency and head from step 5 are within a close tolerance to previous results, end the process.
10. If step 9 was not close enough, repeat steps 7, 8, and 9.

$$P_{Mid} = (P_S \times P_D)^{0.5} \quad \text{(Initial Value)} \tag{49}$$

$$T_{Mid} = (T_S \times T_D)^{0.5} \quad \text{(Initial Value)} \tag{50}$$

$$a = Z_S - b \tag{51}$$

$$b = \frac{(Z_S + Z_D - 2 \times Z_{Mid})}{[(P_D/P_S)^{0.5} - 1]^2} \tag{52}$$

$$c = \frac{Z_D - a - b(P_D/P_S)}{LN(P_D/P_S)} \tag{53}$$

$$\frac{1}{\eta_{Poly}} = 1 + \frac{(S_D - S_S)/\,R}{aLN(P_D/P_S) + b[(P_D/P_S) - 1] + \left(\frac{c}{2}\right)[LN(P_D/P_S)]^2} \tag{54}$$

$$Head_{Poly} = (H_D - H_S) \times \eta_{Poly} \tag{55}$$

$$d = \frac{a}{2}LN(P_D/P_S) + b[(P_D/P_S)^{0.5} - 1] + \frac{c}{8}[LN(P_D/P_S)]^2 \tag{56}$$

$$e = aLN(P_D/P_S) + b[(P_D/P_S) - 1] + \frac{c}{2}[LN(P_D/P_S)]^2 \tag{57}$$

$$S_{Mid\ new} = S_S + (S_D - S_S)\,{}^{d}/_{e} \quad \text{(Recursive)} \tag{58}$$

$$T_{Mid\ new} = T_{Mid\ prev} \times exp\left[\left(S_{Mid\ new} - S_{Mid\ prev}\right)/C_P\right] \quad \text{(Recursive)} \tag{59}$$

Small Stage Stepped Numerical Method

1. Determine an initial estimate of polytropic efficiency by the Schultz 1 method.
2. Select a number of equal pressure ratio steps i between suction and discharge and calculate the pressure ratio using Equation (14).
3. Determine isentropic conditions H_{iseni} at a step by using the step pressure P_i and the entropy from the previous step, $S_{isen\ i-1}$ using an equation of state.
4. Calculate the change in isentropic enthalpy between step i and step i-1.
5. Divide the result of step 4 by the assumed efficiency to get the polytropic change in enthalpy ΔH_i at step i.
6. Add the result of step 5 to the polytropic enthalpy from step i-1.
7. Use the result of step 6 and the step pressure P_i to get polytropic entropy and discharge temperature T_i at step i using an equation of state.
8. Repeat steps 3, 4, 5, 6, and 7 for all steps.
9. Compare the final polytropic discharge temperature to the given discharge temperature.

10. If the results of step 9 are within an acceptably small tolerance, sum up the values of H_{iseni} and H_i from steps 3 and 5 using Equation (13)
11. If the results of step 9 are not within tolerance increment polytropic efficiency and repeat steps 3, 4, 5, 6, 7, 8, 9, and 10 until the tolerance is met.
12. Also, see Evans and Huble (2017) for an expanded spreadsheet version of this method's implementation description.

Sandberg and Colby Method (Modified Schultz 1 Correction Factor)

1. Follow the same process as for the Schultz 1 Method above with the following exceptions.
2. Calculate T_{avg} from Equation (60) (use temperature in degrees Rankine)
3. Use Equation (42) in steps 4 and 6 of the Schultz 1 method.

$$Average\ Temperature = T_{Avg} = \frac{(T_D + T_S)}{2} \tag{60}$$

$$Sandberg\ Colby\ Polytropic\ Correction\ Factor = f_{sc} = \frac{(H_D - H_S) - T_{Avg}(S_D - S_S)}{\left(n/n - 1\right)[(P_D v_D) - (P_S v_S)]} \tag{42}$$

Sandberg and Colby Stepped Numerical Integration Method

1. Determine an initial estimate of polytropic efficiency by the Schultz 1 method.
2. Select a number of equal pressure ratio steps i between suction and discharge and calculate the pressure ratio using Equation (14).
3. Using segment inlet conditions and outlet pressure and isentropic outlet temperature, calculate segment head, enthalpy change and efficiency using the Schultz method and Equation (2)
4. Iterate segment outlet temperature to match assumed efficiency
5. Move to next segment using outlet conditions of previous segment as inlet conditions
6. Repeat steps 3, 4, and 5 for each segment
7. Compare final discharge temperature with given value
8. If step 7 result is not within a small tolerance, iterate efficiency and repeat steps 3, 4, 5, 6, and 7 until agreement is reached within the tolerance
9. Sum up values for head and enthalpy change.
10. Validate final efficiency assumed is equal to ratio of items in step 9

Nathoo and Gottenberg Stepped Numerical Method (not implemented in this paper's results)

1. Assume a polytropic efficiency as a constant value along the path.
2. Numerically integrate Equations (35) and (36) from suction to discharge pressure. (No details given)
3. Compare calculated discharge temperature to measured value.
4. If final temperature is not within a small tolerance of the measured value, select a new polytropic efficiency.
5. Repeat steps 2 and 3 until step 4 is satisfied.
6. Results are stepped values of P, V, and a polytropic efficiency
7. A method to predict efficiency increments and number of pressure steps was not specified
8. Knowing P and V along the compression path, the numerator in Equation (1) can be evaluated.
9. Use Equation (1) to calculate polytropic efficiency, η_{poly}, by dividing result of step 8 by ($H_D - H_S$).

Oldrich Stepped Numerical Methods (not implemented in this paper's results)

For the first application Oldrich used the Merson modification of the Runge Kutta method to iterate density after selecting an initial value for the required accuracy in discharge density and an initial step size. The Merson modified method for Runge Kutta then controls step sizes to accommodate the allowed final error.

1. Given suction pressure and temperature, discharge temperature, polytropic efficiency, and gas composition
2. Select an equation of state that can calculate the variables based upon temperature and density.
3. Assume polytropic efficiency is a constant value along the path.
4. Numerically integrate Equation (38) from suction to discharge conditions.
5. Calculate remaining discharge values with Equation (41)

The solution technique is slightly modified for the second application and is seeded with an initial estimate of polytropic efficiency from the Schultz method and becomes iterative after the initial step size for the Merson modified Runge Kutta method is determined.

The third application (compressor testing) is applicable for this paper:

1. Assume a polytropic efficiency as a constant value along the path.
2. Use the Schultz method to get an initial efficiency estimate.
3. Use the Mallen and Saville method to obtain a second result.
4. Solve Equation (38) with each of these two polytropic efficiency estimates to get two estimated discharge pressures.
5. Using these two discharge pressures make a linear interpolation or extrapolation to estimate a new polytropic efficiency.
6. Solve Equation (38) with this third polytropic efficiency estimate to get a third estimated discharge pressure.
7. Use a second order polynomial curve fit of these three results to predict the next polytropic efficiency.
8. Solve Equation (38) with this fourth polytropic efficiency estimate to get a fourth estimated discharge pressure.
9. Repeat steps 7 and 8 updating the polynomial curve fit until an acceptably low difference between successive polytropic efficiency results is found.
10. Results are stepped values of P, V, and a polytropic efficiency
11. Knowing P and V along the compression path, the numerator in Equation (1) can be evaluated.

Wettstein Stepped Numerical Method (not implemented in this paper's results)
Wettstein used equal pressure ratio steps applied to Equation (11) from suction to discharge pressure. For each step he evaluated the volume based upon the step pressure and an average temperature.

1. Select a number of pressure steps of equal ratio between suction and discharge.
2. Estimate initial efficiency.
3. Increment pressure P_i and estimate a temperature, T_i, at the next step.
4. Calculate an average temperature $T_{avg} = (T_i + T_{i-1}) / 2$.
5. Calculate V_i, H_i, S_i based upon P_i and estimated T_{avg}.
6. Iterate temperature T_i for the step until the change in enthalpy (H_i-H_{i-1}) times the estimated efficiency equals the volume (V_i) times the change in pressure (Pi-P_1) within a small tolerance.
7. Repeat steps 3, 4, 5, and for all pressure increments.
8. Compare the final discharge temperature to the given value, T_D.
9. Increment efficiency and repeat steps 3, 4, 5, 6, 7, and 8, until the final discharge temperature error is within a given small tolerance.
10. Knowing efficiency and (H_D – H_S), calculate $Head_{Poly}$ from Equation (1).

APPENDIX C – EXAMPLE CASE INPUTS AND RESULTS

Table 6: Fluid Compositions for Examples

	Example Identifiers															
	Schultz	Hunt 2, 3 Eth 1-9	SC A, B, C, D, E, F	SC G, H, I	SC J, K, L	SC M, N, O, P, Q, R	SC S, T, U	SC V, W, X	SC Y, Z, AA, AB, AC, AD	SC AE, AF, AG	SC AH, AI, AJ	SC AK, AL, AM, AX, AY	SC AN, AO, AP, AQ, AR, AS, AW	SC AT, AU, AV, Hunt 4	CO2 Inj1 - Inj5	Plano dry
Methane			50	25.6274	60.4842	68.8671	74.2574	85.8644	80.40	18.579	30.2940	30	100		5	94.3334
Ethane				2.2871	5.5619	11.9957	7.4107	11.5319	5.35	1.5920	3.7480					3.0885
Propane				0.5691	1.5369	10.2964	9.7710	0.4501	1.69	37.966	43.5330					1.2458
isoButane				0.0001	0.0010	3.1432	1.5802	0.0001	0.11	0.0884	0.2220					0.2376
Butane				0.0001	0.0010	2.7541	3.9704	0.0001	0.17	0.3071	0.2180					0.3372
n-Pentane				0.0001	0.0010	0.8927	0.6701		0.02	0.0134						0.1044
i-Pentane				0.0001	0.0010	0.5563	0.5301		0.01	0.0884						0.1121
n-Hexane				0.0175	0.0551		0.1800									
Nitrogen				0.2629	0.6933	0.2477	0.2400	0.6601	0.61	0.0657	0.3990					0.3169
Carbon dioxide			50	71.2356	31.6646	1.2468	1.3901	1.4903	11.64	41.300	21.5860	70		100	95	0.2240
Ethylene		100														
H2S								0.0030								
R12	100															

Mole Weight	120.91	28.05	30.03	36.49	26.23	24.29	23.38	18.28	20.73	38.70	35.05	35.62	16.04	44.01	42.61	17.29
Critical Pressure (psia)	599.89	731.25	1260.72	1232.25	1093.23	1529.52	1588.69	893.07	949.87	1102.88	1160.03	1287.60	667.06	1069.99	1128.79	899.02
Critical Temp. (°F)	233.55	48.56	-4.90	44.30	-27.97	41.50	26.48	-72.70	-64.25	110.32	111.73	38.80	-116.6	87.76	81.50	-85.50

Compositions are given in molar volume %.
Critical property values provided by REFPROP software (Lemmon, et al. 2013).

Table 7: Example Inputs and Errors Compared to a Reference Small Stage 100 Step Method

	Stagnation Properties*				Small Stage 100 Step		Errors from Small Stage 100-Step (%)										
Example Case	P1 (psia)	P2 (psia)	T1 (°F)	T2 (°F)	Poly. Head (ft-lbf/lbm)	Poly. Eff. (%)	Schultz	Schultz XY	SC	Mallen Saville	Hunt. 3-Point	SC 20-Step	Hunt. 20 Step	Hunt. 50 Step	Hunt. 350 Step	Small Stage 20-Step	Small Stage 50-Step
Schultz	10.0	130.0	-10.00	210.0	17289	75.01	0.247	0.020	-0.313	0.125	0.023	-0.022	-0.111	-0.034	-0.019	-0.208	-0.052
Hunt 2	362.5	7250.0	98.30	566.3	118500	80.56	-1.795	15.563	0.178	0.892	-0.199	0.015	-0.040	-0.012	-0.007	-0.253	-0.063
Hunt 3	362.5	4351.2	98.30	503.3	90920	75.07	-1.532	7.081	-0.032	0.769	-0.130	0.017	-0.027	0.000	0.005	-0.301	-0.075
Hunt 4	1100.1	6000.3	98.30	368.3	26866	64.29	-1.349	0.779	0.464	1.168	0.115	0.035	0.037	0.026	0.024	-0.373	-0.094
SC A	1500.0	5364.3	90.00	291.3	34810	82.02	-0.356	0.687	0.120	0.295	-0.030	-0.036	-0.035	-0.040	-0.040	-0.124	-0.032
SC B	1500.0	6738.8	90.00	331.0	44000	82.04	-0.481	1.048	0.179	0.415	-0.036	-0.028	-0.026	-0.032	-0.034	-0.140	-0.034
SC C	1500.0	7496.2	90.00	350.0	48751	82.05	-0.541	1.232	0.209	0.476	-0.039	-0.025	-0.023	-0.030	-0.032	-0.149	-0.037
SC D	1700.0	6685.9	70.00	259.2	34809	82.02	-0.358	0.356	0.205	0.373	-0.018	-0.036	-0.032	-0.039	-0.040	-0.120	-0.030
SC E	1700.0	8359.2	70.00	294.5	44000	82.05	-0.447	0.459	0.275	0.497	-0.016	-0.029	-0.024	-0.033	-0.035	-0.135	-0.033
SC F	1700.0	9266.9	70.00	311.5	48755	82.03	-0.490	0.494	0.310	0.560	-0.016	-0.026	-0.021	-0.032	-0.034	-0.144	-0.036
SC G	1649.7	8189.7	101.20	316.2	34807	82.08	-0.410	0.614	0.298	0.485	-0.023	-0.036	-0.026	-0.036	-0.038	-0.127	-0.032
SC H	1649.7	10388.1	101.20	354.0	44001	82.06	-0.487	0.698	0.382	0.627	-0.019	-0.026	-0.019	-0.032	-0.035	-0.144	-0.037
SC I	1649.7	11577.4	101.20	372.1	48756	82.04	-0.521	0.717	0.424	0.698	-0.016	-0.023	-0.015	-0.030	-0.033	-0.151	-0.038
SC J	3138.6	8615.6	98.50	223.4	34807	82.05	-0.145	-0.192	0.124	0.198	0.015	-0.049	-0.046	-0.050	-0.051	-0.075	-0.019
SC K	3138.6	10273.4	98.50	248.8	44002	82.01	-0.188	-0.274	0.165	0.268	0.017	-0.045	-0.041	-0.046	-0.047	-0.088	-0.021
SC L	3138.6	11157.3	98.50	261.2	48758	81.99	-0.211	-0.322	0.185	0.303	0.016	-0.045	-0.041	-0.046	-0.047	-0.095	-0.024
SC M	868.8	2405.3	124.90	267.1	34810	82.04	-0.156	0.784	0.023	0.109	-0.017	-0.045	-0.052	-0.048	-0.048	-0.085	-0.021
SC N	868.8	3002.5	124.90	298.8	44006	82.04	-0.269	1.494	0.047	0.170	-0.030	-0.039	-0.048	-0.044	-0.044	-0.101	-0.025
SC O	868.8	3342.7	124.90	314.1	48757	82.07	-0.335	1.946	0.062	0.204	-0.039	-0.037	-0.048	-0.044	-0.043	-0.110	-0.028
SC P	1891.3	5438.2	120.00	238.3	34810	82.05	-0.213	0.313	0.159	0.222	-0.013	-0.049	-0.047	-0.052	-0.053	-0.073	-0.019
SC Q	1891.3	6576.0	120.00	260.5	44006	82.03	-0.270	0.422	0.218	0.303	-0.012	-0.043	-0.041	-0.047	-0.049	-0.082	-0.020
SC R	1891.3	7188.6	120.00	271.1	48758	82.04	-0.296	0.469	0.247	0.343	-0.012	-0.042	-0.038	-0.046	-0.047	-0.087	-0.021
SC S	1319.0	3736.5	110.00	247.3	34810	82.06	-0.249	0.876	0.108	0.192	-0.034	-0.043	-0.045	-0.048	-0.048	-0.084	-0.021
SC T	1319.0	4589.4	110.00	274.6	44006	82.03	-0.353	1.404	0.161	0.278	-0.048	-0.038	-0.040	-0.044	-0.045	-0.099	-0.025
SC U	1319.0	5059.7	110.00	287.6	48760	82.04	-0.403	1.689	0.191	0.324	-0.053	-0.036	-0.038	-0.042	-0.043	-0.105	-0.026
SC V	2138.0	4485.2	110.00	222.8	34814	82.01	-0.125	0.056	0.058	0.117	0.001	-0.051	-0.051	-0.053	-0.053	-0.070	-0.018
SC W	2138.0	5235.1	110.00	247.4	44008	82.04	-0.184	0.119	0.084	0.169	-0.001	-0.047	-0.047	-0.049	-0.050	-0.083	-0.021
SC X	2138.0	5641.5	110.00	259.5	48763	82.02	-0.215	0.157	0.099	0.198	-0.001	-0.045	-0.044	-0.047	-0.047	-0.089	-0.022
SC Y	537.0	1288.7	59.00	197.9	34813	82.02	-0.048	0.061	-0.038	0.065	0.000	-0.048	-0.053	-0.049	-0.049	-0.091	-0.024
SC Z	537.0	1570.1	59.00	232.0	44005	82.06	-0.091	0.147	-0.054	0.097	0.001	-0.043	-0.050	-0.045	-0.044	-0.110	-0.028
SC AA	537.0	1730.9	59.00	249.2	48757	82.06	-0.117	0.214	-0.060	0.116	0.002	-0.039	-0.047	-0.041	-0.040	-0.118	-0.029
SC AB	1754.8	5275.5	20.00	149.7	34809	82.02	-0.230	-0.036	0.149	0.253	-0.004	-0.044	-0.042	-0.047	-0.048	-0.095	-0.025
SC AC	1754.8	6392.3	20.00	175.2	44004	82.02	-0.296	-0.061	0.202	0.344	0.000	-0.039	-0.035	-0.042	-0.043	-0.108	-0.027
SC AD	1754.8	6992.7	20.00	187.5	48755	82.03	-0.328	-0.079	0.229	0.390	0.001	-0.036	-0.032	-0.039	-0.041	-0.114	-0.028
SC AE	335.0	1695.8	100.00	311.7	34803	82.04	-0.158	2.178	-0.105	0.082	-0.021	-0.035	-0.065	-0.042	-0.038	-0.126	-0.031
SC AF	335.0	2416.6	100.00	361.4	43994	82.05	-0.425	4.885	-0.114	0.151	-0.047	-0.026	-0.068	-0.039	-0.033	-0.152	-0.039
SC AG	335.0	2862.0	100.00	385.1	48746	82.04	-0.598	6.792	-0.101	0.204	-0.063	-0.019	-0.066	-0.035	-0.029	-0.162	-0.040
SC AH	2071.0	8172.4	160.00	272.0	34814	82.02	-0.143	-0.416	0.208	0.258	0.008	-0.052	-0.047	-0.054	-0.055	-0.062	-0.016
SC AI	2071.0	10025.7	160.00	291.9	44009	82.06	-0.165	-0.608	0.263	0.330	0.006	-0.048	-0.042	-0.050	-0.052	-0.070	-0.017
SC AJ	2071.0	11010.8	160.00	301.5	48762	82.06	-0.174	-0.712	0.289	0.365	0.004	-0.047	-0.040	-0.049	-0.051	-0.075	-0.018

Table 7: Example Inputs and Errors Compared to a Reference Small Stage 100 Step Method (Cont'd)

	Stagnation Properties*				Small Stage 100 Step		Errors from Small Stage 100-Step (%)										
Example Case	P1 (psia)	P2 (psia)	T1 (°F)	T2 (°F)	Poly. Head (ft-lbf/lbm)	Poly. Eff. (%)	Schultz	Schultz XY	SC	Mallen Saville	Hunt. 3-Point	SC 20-Step	Hunt. 20 Step	Hunt. 50 Step	Hunt. 350 Step	Small Stage 20-Step	Small Stage 50-Step
SC AK	1000.0	4264.3	100.00	349.2	34805	82.04	-0.400	1.371	0.027	0.271	-0.038	-0.027	-0.033	-0.032	-0.032	-0.144	-0.035
SC AL	1000.0	5571.9	100.00	400.5	43997	82.03	-0.595	2.261	0.068	0.398	-0.059	-0.019	-0.027	-0.028	-0.028	-0.169	-0.042
SC AM	1000.0	6312.6	100.00	425.0	48748	82.04	-0.690	2.748	0.094	0.467	-0.069	-0.017	-0.024	-0.026	-0.026	-0.179	-0.045
SC AN	1000.0	1891.1	100.00	209.4	34809	82.09	-0.036	0.022	-0.006	0.052	0.003	-0.052	-0.054	-0.053	-0.052	-0.067	-0.016
SC AO	1000.0	2190.6	100.00	236.3	44008	82.07	-0.068	0.055	-0.010	0.076	0.003	-0.048	-0.051	-0.049	-0.049	-0.082	-0.020
SC AP	1000.0	2356.4	100.00	249.9	48764	82.03	-0.087	0.081	-0.012	0.091	0.003	-0.047	-0.050	-0.048	-0.047	-0.090	-0.022
SC AQ	3000.0	5596.5	100.00	194.4	34811	82.12	-0.082	-0.042	0.049	0.094	0.008	-0.053	-0.052	-0.053	-0.054	-0.057	-0.013
SC AR	3000.0	6381.1	100.00	215.6	44008	82.07	-0.123	-0.055	0.068	0.132	0.007	-0.051	-0.050	-0.052	-0.052	-0.070	-0.018
SC AS	3000.0	6800.8	100.00	226.1	48763	82.04	-0.145	-0.061	0.078	0.153	0.007	-0.049	-0.048	-0.051	-0.051	-0.076	-0.019
SC AT	1000.0	6923.9	100.00	407.3	34802	82.04	-0.769	3.926	0.269	0.608	-0.193	-0.011	-0.015	-0.024	-0.026	-0.175	-0.044
SC AU	1000.0	9222.4	100.00	459.9	43996	82.01	-0.924	5.105	0.385	0.818	-0.203	-0.002	-0.004	-0.017	-0.020	-0.195	-0.048
SC AV	1000.0	10492.7	100.00	484.6	48747	82.01	-0.986	5.592	0.440	0.917	-0.206	-0.001	-0.001	-0.016	-0.019	-0.206	-0.052
SC AW	100.0	300.0	100.00	290.0	68428	81.65	-0.082	-0.069	-0.059	0.101	0.013	-0.043	-0.052	-0.044	-0.043	-0.108	-0.027
SC AX	800.0	2400.0	100.00	290.0	25694	81.12	-0.142	0.402	-0.043	0.122	-0.006	-0.038	-0.043	-0.040	-0.039	-0.121	-0.030
SC AY	2000.0	6000.0	100.00	230.0	20575	81.16	-0.193	-0.076	0.156	0.240	0.017	-0.047	-0.044	-0.049	-0.050	-0.090	-0.024
Eth 1	21.5	52.1	97.16	217.6	29850	80.21	-0.055	-0.020	-0.004	0.075	0.005	-0.050	-0.057	-0.051	-0.050	-0.077	-0.019
Eth 2	47.6	90.6	98.60	195.4	21164	72.27	-0.042	-0.023	-0.004	0.078	0.001	-0.048	-0.051	-0.048	-0.047	-0.090	-0.022
Eth 3	88.0	162.0	94.28	181.9	19401	75.81	-0.025	-0.012	-0.003	0.055	-0.001	-0.052	-0.055	-0.052	-0.051	-0.072	-0.018
Eth 4	152.1	274.4	106.88	186.4	18600	82.87	-0.009	0.001	-0.001	0.029	-0.002	-0.058	-0.061	-0.058	-0.057	-0.045	-0.010
Eth 5	265.0	472.8	92.66	185.0	17113	68.35	-0.017	0.007	-0.012	0.080	-0.003	-0.041	-0.044	-0.041	-0.041	-0.106	-0.025
Eth 6	460.0	782.0	93.00	170.0	13985	79.71	-0.003	0.039	-0.005	0.031	-0.004	-0.053	-0.055	-0.053	-0.053	-0.056	-0.012
Eth 7	765.0	1262.3	93.00	165.0	10728	79.02	-0.039	0.090	0.015	0.048	-0.005	-0.049	-0.051	-0.050	-0.050	-0.056	-0.010
Eth 8	1245.0	1992.0	93.00	160.0	6461	67.88	-0.076	-0.092	0.079	0.098	0.077	-0.049	-0.048	-0.050	-0.050	-0.054	-0.009
Eth 9	21.5	472.8	97.16	250.0	129394	82.21	-0.383	0.953	-0.146	0.445	0.032	-0.022	-0.125	-0.035	-0.018	-0.208	-0.052
Plano dry	638.2	1697.0	77.00	241.6	50003	80.08	-0.095	0.087	-0.043	0.105	0.002	-0.042	-0.047	-0.043	-0.043	-0.114	-0.029
CO2 inj1	25.0	120.0	85.00	365.0	37621	85.22	-0.076	0.034	-0.110	0.102	0.017	-0.042	-0.062	-0.045	-0.041	-0.114	-0.028
CO2 inj2	110.0	370.0	100.00	350.0	29002	67.50	-0.114	0.021	-0.295	0.248	0.031	-0.008	-0.016	-0.009	-0.007	-0.248	-0.061
CO2 inj3	350.0	1160.0	100.00	360.0	26940	62.69	-0.140	0.105	-0.394	0.322	0.024	0.008	0.002	0.008	0.009	-0.321	-0.081
CO2 inj4	1150.0	3500.0	100.00	275.0	16164	63.54	-0.669	0.123	0.160	0.511	0.098	0.005	0.006	0.002	0.001	-0.270	-0.066
CO2 inj5	3490.0	6500.0	100.00	150.0	8304	56.19	0.055	0.057	0.012	0.060	0.089	-0.044	-0.044	-0.044	-0.044	-0.082	-0.017

* See Appendix A of ASME PTC 10 (1997) for a discussion of using stagnation conditions to define compressor performance.

Example input data sources include: Schultz (1962), Huntington (1985), Sandberg and Colby (2013), and Plano (2014)

REFERENCES

Aicher, W., 1993, "Test of Process Turbocompressors without CFC Gases," Proceedings of the 22nd Turbomachinery Symposium, Turbomachinery Laboratory, Texas A&M University, College Station, Texas, pp. 179-184.

API Standard 617, 2014, "Axial and Centrifugal Compressors and Expander-Compressors," Eighth Edition, American Petroleum Institute, Washington, D.C.

ASME PTC 10, 1949, "Power Test Code for Centrifugal, Mixed Flow, and Axial Flow Compressors and Exhausters," American Society of Mechanical Engineers, New York, NY.

ASME PTC 10, 1965, "Compressors and Exhausters Power Test Code 10," American Society of Mechanical Engineers, New York, NY.

ASME PTC 10, 1997, "Performance Test Code on Compressors and Exhausters," American Society of Mechanical Engineers, New York, NY.

Assael M. J., Trusler, J. P. M. and Tsolakis, T. F., 1996, Thermophysical Properties of Fluids: An Introduction to Their Prediction, Singapore, Singapore: World Scientific Publishing Co. Pte. Ltd.

Benedict, M., Webb, G. B., Rubin, L. C., 1940, "An Empirical Equation for Thermodynamic Properties of Light Hydrocarbons and their Mixtures," J. Chem. Physics, 8, pp. 334-345.

Benedict, M., Webb, G. B., Rubin, L. C., 1942, "An Empirical Equation for Thermodynamic Properties of Light Hydrocarbons and their Mixtures II. Mixtures of Methane, Ethane, Propane, and n-Butane," J. Chem. Physics, 10, pp.757-758.

Boyce, M. P., 1972, "New Developments in Compressor Aerodynamics," Proceedings of the First Turbomachinery Symposium, Turbomachinery Laboratory, Texas A&M University, College Station, Texas, pp. 79-89.

Boyce, M. P., 1993, "Principals of Operation and Performance Estimation of Centrifugal Compressors," Proceedings of the 22nd Turbomachinery Symposium, Turbomachinery Laboratory, Texas A&M University, College Station, Texas, pp. 161-177.

Boyce, M. P., Bayley, R. D., Sudhakar, V., and Elchuri, V., 1976, "Field Testing of Compressors," Proceedings of the Fifth Turbomachinery Symposium, Turbomachinery Laboratory, Texas A&M University, College Station, Texas, pp. 149-159.

Box, G. E. and Draper, N.R., 1987, Empirical Model-Building and Response Surfaces, Hoboken, New Jersey, Wiley.

Brenne, L., Bjorge, T., Gilarranz, J. L., and Miller, H., 2005, "Performance Evaluation of a Centrifugal Compressor Operating Under Wet Gas Conditions," Proceedings of the 34th Turbomachinery Symposium, Turbomachinery Laboratory, Texas A&M University, College Station, Texas, pp. 111-120.

Brown, R. N., 1997, Compressors Selection and Sizing, Second Edition, Woburn, Massachusetts, Butterworth-Heinemann.

Brown, R. N. and Lewis, R. A., 1994, "Centrifugal Compressor Application Sizing, Selection, and Modeling," Proceedings of the 23rd Turbomachinery Symposium, Turbomachinery Laboratory, Texas A&M University, College Station, Texas, pp. 195-201.

Burgh, N. P., 1869, The Indicator Diagram Practically Considered," London, United Kingdom: E. & F.N. Spon.

Clark, W. A., 1981, "Measure Power by the Simplest Method and Use for Onstream Computer Monitoring," Proceedings of the Tenth Turbomachinery Symposium, Turbomachinery Laboratory, Texas A&M University, College Station, Texas, pp. 151-153.

Colby, G. M., 2005, "Hydraulic Shop Performance testing of Centrifugal Compressors," Proceedings of the 34th Turbomachinery Symposium, Turbomachinery Laboratory, Texas A&M University, College Station, Texas, pp.147-154.

Cumpsty, Nicholas A., 1989, Compressor Aerodynamics, Longman Scientific and Technical Group, UK.

Davis, H. M., 1973, "Compressor Performance, Field Data Acquisition and Evaluation," Proceedings of the Second Turbomachinery Symposium, Turbomachinery Laboratory, Texas A&M University, College Station, Texas, pp. 143-146.

Duggan, J. B., 1987, "Compressor Performance Modelling and Monitoring," Proceedings of the 16th Turbomachinery Symposium, Turbomachinery Laboratory, Texas A&M University, College Station, Texas, pp. 9-21.

Dzung, L. S., 1944, "Beitrage zur Thermodynamik der realen Gase," Schweizer Arch.10 (1944) S. 305/13.

Evans, B. F. and Huble, S. R., 2017, Centrifugal Compressor Polytropic Performance: Consistently Accurate Results From Improved Real Gas Calculations, Proceedings of ASME GT2017, Paper Number 65235, ASME Turbo Expo 2017.

Girdhar, P., 2008, Performance Evaluation of Pumps and Compressors, Raleigh, North Carolina, USA: Lulu.com.

Goodwin, A. R., Sengers, J. V., Peters, C. J., 2010, Applied Thermodynamics of Fluids, Cambridge, UK: The Royal Society of Chemistry.

Hunt, J. W., 1981, "Field Testing of Centrifugal Compressors," Proceedings of the Tenth Turbomachinery Symposium, Turbomachinery Laboratory, Texas A&M University, College Station, Texas, pp. 157-160.

Huntington, R. A., 1985, "Evaluation of Polytropic Calculation Methods for Turbomachinery Performance," ASME Transactions, Journal of Engineering for Gas Turbines and Power, 107, pp. 872-879.

Huntington, R., 1997, "Limitations of the Schultz Calculation for Polytropic Head - A Proposal for Revision of PTC-10," Technical Report [Online], DOI: 10.13140/RG.2.1.2088.4087,
https://www.researchgate.net/publication/304251146_LIMITATIONS_OF_THE_SCHULTZ_CALCULATION_FOR_POLYTROPIC_HEAD_-A_PROPOSAL_FOR_REVISION_OF_PTC-10

Hundseid, O., Bakken, L. E. and Helde, T., 2006, "A Revised Compressor Polytropic Performance Analysis," Proceedings of ASME GT2006, Paper Number 91033, ASME Turbo Expo 2006.

Hundseid, O. and Bakken, L. E., 2006, "Wet Gas Performance Analysis," Proceedings of ASME GT2006, Paper Number 91035, ASME Turbo Expo 2006.

Jacobsen, R. T. and Stewart, R. B., 1973, "Thermodynamic Properties of Nitrogen Including Liquid and Vapor Phases from 63 to 2000 °K with Pressures up to 10,000 MPa," J. Phys. Chem. Ref. Data, 2, pp. 757-922.

Jacobsen, R. T. ,Stewart, R. B., Jahangiri, M., 1986, "Thermodynamic Properties of Nitrogen from the Freezing Line to 2000 K at pressures to 1000 MPa," J. Phys. Chem. Ref. Data, 2, pp. 735-909.

Johnson, A. and Johansen, B., 2009, "Comparison of Five Natural Gas Equations of State Used for Flow and Energy Measurement," [Online}, https://www.nist.gov/publications/comparison-five-natural-gas-equations-state-used-flow-and-energy-measurement

Keenan, J. T., Strite, M. A., and Rassmann, F. A., 1998, "Centrifugal Performance Testing – Basics for Testing," Short Course 6 of the 27th Turbomachinery Symposium, Turbomachinery Laboratory, Texas A&M University, College Station, Texas.

Key, B., 1989, "Dynamic Similitude Theory: Key to Understanding the ASME Compressors Performance Test," Proceedings of Society of Petroleum Engineers, Journal of Petroleum Technology, 41, Paper Number 16474-PA, pp. 860-866.

Klein, M. J., 1989, "The Scientific Style of Josiah Willard Gibbs," A Century of Mathematics in America, Part II, Providence, Rhode Island: American Mathematical Society, pp. 99-119.

Kumar, S. K., Kurz, R., O'Connell, J. P., 1999, "Equations of State for Gas Compressor Design and Testing," ASME International Gas Turbine & Aeroengine Congress & Exhibition, Paper Number 99-GT-12.

Kunz, O., Klimeck, R., Wagner, W., and Jaeschke, M., 2007, The GERG-2004 Wide-Range Equation of State for Natural Gases and Other Mixtures, Groupe Europeen de Recherches Gazieres Technical Monograph 15, Verlag des Deutscher Ingenieure: Dusseldorf, Germany.

Kurz, R. and Brun, K., 1997, "Field Testing of Gas Turbine Driven Centrifugal Compressor Packages Test Procedures and Measurement Uncertainties," Proceedings of the 34th Turbomachinery Symposium, Turbomachinery Laboratory, Texas A&M University, College Station, Texas, pp. 53-62.

Kurz, R. and Brun, K., 2005, "Site Performance Test Evaluation for Gas Turbine and Electric Motor Driven Compressors," Proceedings of the 26th Turbomachinery Symposium, Turbomachinery Laboratory, Texas A&M University, College Station, Texas, pp. 19-33.

Kurz, R., Brun, K., and Legrand, D. D., 1999, "Field Performance Testing of Gas Turbine Driven Compressor Sets," Proceedings of the 28th Turbomachinery Symposium, Turbomachinery Laboratory, Texas A&M University, College Station, Texas, pp. 213-230.

Kurz, R. and Brun, K., 2005, "Site Performance Test Evaluation for Gas Turbine and Electric Motor Driven Compressors," Proceedings of the 34th Turbomachinery Symposium, Turbomachinery Laboratory, Texas A&M University, College Station, Texas, pp. 53-62.

Lee B.I., and Kesler M.G., 1975, "A Generalized Thermodynamic Correlation Based on Three-Parameter Corresponding States", AIChE J., 21(3), pp. 510-527.

Lambert, F. L., 2013, "Entropy Is Simple...If You Avoid The Briar Patches!," http://Entropysimple.oxy.edu/content.htm.

Lemmon, E. W., Huber, M. L., and McLinden, M. O., 2013, NIST Standard Reference Database 23: Reference Fluid Thermodynamic and Transport Properties - REFPROP, Version 9.1, National Institute of Standards and Technology, Standard Reference Data Program: Gaithersburg, MD.

Lemmon, E. W. and Span, R., 2010, "Chapter 12: Multi-parameter Equations of State for Pure Fluids and Mixtures," Applied Thermodynamics of Fluids, Royal Society of Chemistry.

Ludtke, K., 1992, "Twenty Years of Experience with a Modular Design System for Centrifugal Process Compressors," Proceedings of the 21st Turbomachinery Symposium, Turbomachinery Laboratory, Texas A&M University, College Station, Texas, pp. 21-34.

Ludtke, K., 1997, "Rerate of Centrifugal Process Compressors – Wider Impellers or Higher Speed or Suction Side Boosting," Proceedings of the 26th Turbomachinery Symposium, Turbomachinery Laboratory, Texas A&M University, College Station, Texas, pp.43-55.

Ludtke, K. H., 2004, Process Centrifugal Compressors: Basics, Function, Operation, Design, Application, Berlin, Germany: Springer-Verlag.

Mallen, M. and Saville, G., 1977, "Polytropic Processes in the Performance Prediction of Centrifugal Compressors," I. Mech. E. Conference Publications C183/77, pp. 89-96.

Maretti, A., Giovannini, M., and Nava, P., 1982, "Shop Full-Load Testing of Centrifugal Compressors," Proceedings of the 11th Turbomachinery Symposium, Turbomachinery Laboratory, Texas A&M University, College Station, Texas, pp. 113-120.

McLinden, M. O., 2009, "Thermodynamic Properties of Propane. I. p-ρ-T Behavior from (265 to 500) K with Pressures to 36 MPa," J. Chem. Eng. Data, 54, pp. 3181-3191.

Miller, D. P., 2011, "The Mysterious Case of James Watt's '1785' Steam Indicator': Forgery or Folklore in the History of an Instrument?" International Journal for the History of Engineering and Technology, 81, pp. 129-150

Nathoo, N. S. and Gottenberg, W. G., 1981, "Measuring the Thermodynamic Performance of Multistage Compressors Operating on Mixed Hydrocarbon Gases," Proceedings of the Tenth Turbomachinery Symposium, Turbomachinery Laboratory, Texas A&M University, College Station, Texas, pp. 15-23.

Nathoo, N. S. and Gottenberg, W. G., 1983, "A New Look at Performance Analysis of Centrifugal Compressors Operating with Mixed Hydrocarbon Gases," ASME Journal of Engineering for Power, 105, pp. 920-926.

Oldrich, J., 2010, "Advanced Polytropic Calculation Method of Centrifugal Compressor," Proceedings of ASME IMECE2010, Paper Number 40931, ASME International Mechanical Engineering Congress and Exposition 2010.

O'Neill, P. P. and Wickli, H. E., 1962, "Predicting Process Gas Performance of Centrifugal Compressors from Air Test Data," Transactions of ASME, Journal of Engineering for Industry, 41, pp. 248-264

Onnes, H. K., 1902, "Expression of the Equation of State of Gases and Liquids by Means of Series," KNAW Proceedings, 4, pp. 125-147.

Pais, R. B. and Jacobik, G. J., 1974, "Field Performance Testing of Centrifugal Compressors," Proceedings of the Third Turbomachinery Symposium, Turbomachinery Laboratory, Texas A&M University, College Station, Texas, pp. 84-90.

Pitzer, K. S., 1955, "The Volumetric and Thermodynamic Properties of Fluids. I. Theoretical Basis and Virial Coefficients," Journal of the American Chemical Society, Volume 77, Number 13, pp. 3427-3433.

Plöcker, U., Knapp, H., and Prausnitz, J., 1978, "Calculation of High-Pressure Vapor-Liquid Equilibria from a Corresponding States Correlation with Emphasis on Asymmetric Mixtures," Industrial Chemical Process Design Development, Volume 17, Number 3, pp 324-332.

Peng, D. Y. and Robinson, D. B., 1976, "A New Two-Constant Equation of State," Ind. Eng. Chem. Fundam. 15, pp. 59-64.

Plano, M., 2014, "Evaluation of Thermodynamic Models used for Wet Gas Compressor Design," Innovative Sustainable Energy Engineering, Norwegian University of Science and Technology.

Rasmussen, P. C. and Kurz, R., 2009, "Centrifugal Compressor Applications – Upstream and Midstream," Proceedings of the 38th Turbomachinery Symposium, Turbomachinery Laboratory, Texas A&M University, College Station, Texas, pp. 169-186.

Redlich, O. and Kwong, N. S., 1949, "On the Thermodynamics of Solutions. V: An Equation of State. Fugacities of Gaseous Solutions," Chem. Rev. 44, pp. 233-243.

Reid, R. C., Prausnitz, J. M., and Poling, B. E., 1987, The Properties of Gases & Liquids, New York, New York: McGraw-Hill.

Sandberg, M. R., 2005, "Equation of State Influences on Compressor Performance Determination," Proceedings of the 34th Turbomachinery Symposium, Turbomachinery Laboratory, Texas A&M University, College Station, Texas, pp. 121-129.

Riazi, M. R. and Mansoori, G. A., 1992, "An Accurate Equation of State for Hydrocarbon Systems," Society of Petroleum Engineers.

Sandberg, M. R., 2005, "Equation of State Influences on Compressor Performance Determination," Proceedings of the 34th Turbomachinery Symposium, Turbomachinery Laboratory, Texas A&M University, College Station, Texas, pp. 121-129.

Sandberg, M. R. and Colby, G. M., 2013, "Limitations of ASME PTC 10 in Accurately Evaluating Centrifugal Compressor Thermodynamic Performance," Proceedings of the 42nd Turbomachinery Symposium, Turbomachinery Laboratory, Texas A&M University, College Station, Texas.

Schultz, J. M., 1962, "The Polytropic Analysis of Centrifugal Compressors," ASME Journal of Engineering for Power, pp. 69-82.

Sengers, J. V. and Sengers, A. L., 1968, "The Critical Region", Chemical and Engineering News, Volume 46, Number 25, pp. 104-121.

Shah, S. and Bartos, J., 1997, "Confirming Centrifugal Compressor Aerodynamic performance Using Limited Test Data Combined with Computational Fluid Dynamic Techniques," Proceedings of the 26th Turbomachinery Symposium, Turbomachinery Laboratory, Texas A&M University, College Station, Texas, pp. 35-41.

Soave, G. S., 1972, "Equilibrium Constants from a Modified Redlich-Kwong Equation of State," Chem. Eng. Sci. 27, pp. 1197-1203.

Sorokes, J., 2013, "Range Versus Efficiency – Striking the Proper Balance," Proceedings of the Forty-Second Turbomachinery Symposium, Turbomachinery Laboratory, Texas A&M University, Houston, Texas, pp. 123-130.

Sorokes, J. M., Kuzdzal, M. J., Sandberg, M. R., and Colby, G. M., 1994, "Recent Experiences in Full Load Full Pressure Shop Testing of a High Pressure Gas Injection Centrifugal Compressor," Proceedings of the 23rd Turbomachinery Symposium, Turbomachinery Laboratory, Texas A&M University, College Station, Texas, pp. 3-17.

Sorokes, J. M., Memmott, E. A., Kaulius, S. T., 2014, "Revamp / Rerate Design Considerations," Proceedings of the 43rd Turbomachinery Symposium, Turbomachinery Laboratory, Texas A&M University, College Station, Texas.

Span, R., 2000, Multiparameter Equations of State: An accurate Source of Thermodynamic Property Data, New York, New York: Springer.

Span, R. and Lemmon, E.W., 2015, "Chapter 5: Volumetric Properties from Multiparameter Equations of State," Volume Properties: Liquids, Solutions and Vapours, Royal Society of Chemistry.

Stanley, R. A. and Bohannan, W. R., 1977, "Dynamic Simulation of Centrifugal Compressor Systems," Proceedings of the Sixth Turbomachinery Symposium, Turbomachinery Laboratory, Texas A&M University, College Station, Texas, pp. 123-130.

Starling, K. E., 1973, Fluid Thermodynamic Properties for Light Petroleum Systems. Houston, Texas: Gulf Publishing.

Stodola, A., 1910, Die Dampfturbine Mit einem Anhang uber die Aussichten der Warmekraftmaschinen und die Gasturbine, 4th Edition, Berlin, Germany: Verlag von Julius Springer.

Taher, M., 2014, "ASME PTC-10 Performance Testing of Centrifugal Compressors – The Real Gas Calculation Method," Proceedings of ASME GT2014, Paper Number 26411, ASME Turbo Expo 2014.

Tarpey, T., 2009, "All Models are Right…most are useless," [Online] <http://andrewgelman.com/wp-content/uploads/2012/03/tarpey.pdf>

Thompson, W. E., 1972, "Aerodynamics of Turbines," Proceedings of the First Turbomachinery Symposium, Turbomachinery Laboratory, Texas A&M University, College Station, Texas, pp. 90-104

Turns, S. R., 2006, Thermodynamics Concepts and Applications, New York, New York: Cambridge University Press.

Van der Waals, J. D., 1873, "Over de Continuiteit van den Gas-en. [On the Continuity of the Gas and Liquid State]," Thesis, Univ. Leiden.

van der Waals, J. D., 1910, "The Equation of State for Gases and Liquids," Nobelprize.org, <http://www.nobelprize.org/nobel_prizes/physics/laureates/1910/waals-lecture.html>

Walas, S. M., 1985, Phase Equilibria in Chemical Engineering, Boston, Massachusetts: Butterworth Publishers.

Wettstein, H. E., 2014, "Polytropic Change of State Calculations," Proceedings of ASME IMECE2014, Paper Number 36202, ASME International Mechanical Engineering Congress and Exposition 2014.

Wilcox, E., 1999, "Practical Methods for Field Performance Testing Centrifugal Compressors," Proceedings of the 28th Turbomachinery Symposium, Turbomachinery Laboratory, Texas A&M University, College Station, Texas, pp. 165-177.

"Write in the margins", 2013, Ivy League Student Aid & Testing Services, <http://www.ivyleaguesats.com/2013/10/14/write-in-the-margins/>

Xi, G., Zhang, B., Liang, F., Jiang, H., 2009, "Investigation of the Calculation Model of Polytropic Head for Real Gases," J. of Eng. Thermophysics, 30(11). (In Chinese)

Zeuner, G. A., 1905, Technische Thermodynamik, Leipzig, Germany: Verlag von Arthur Felix.

Zeuner, G. A., 1906, Technical Thermodynamics, Vol. 1, Fundamental Laws of Thermodynamics Theory of Gases, New York, New York: D. Van Nostrand Company.

DISCLAIMER

This paper contains technical interpretations concerning calculations of centrifugal compressor performance. These are intended for informational purposes only. Readers should verify applicability to their individual situations.

ACKNOWLEDGMENTS

The authors would like to thank Chiyoda International Corporation for permission to publish this paper.